8-2012

Enzyme Actuated Bioresponsive Hydrogels

Andrew Wilson
Clemson University, anwilso@clemson.edu

ENZYME ACTUATED BIORESPONSIVE HYDROGELS

A Thesis
Presented to
the Graduate School of
Clemson University

In Partial Fulfillment
of the Requirements for the Degree
Master of Science
Chemical Engineering

---

by
Andrew Nolan Wilson
August 2012

Accepted by:
Dr. Anthony Guiseppi-Elie, Committee Chair
Dr. Mark Roberts
Dr. Christopher Kitchens

ACKNOWLEDGEMENTS

I would like to thank my advisor, Prof. Guiseppi-Elie, for introducing me to the field of biologically responsive smart materials and for giving me the opportunity to work on this project.

This research would not have been possible without his guidance, encouragement, and countless hours of brainstorming with my lab mates Christian Kotanen, Olukayode Karunwi and my undergraduate students Ruth Salas and Hanna Aucoin.

I wish to thank the members of my master's thesis examining committee, Dr. Christopher Kitchens and Dr. Mark Roberts, as well as the Department of Chemical and Biomolecular Engineering.

I would also like to thank Prof. Guiseppi-Elie (ChBE) and Prof. Robert Latour (BioE) for their classroom instruction in transport phenomena that stimulated my interest in this area and exposed me to the many possibilities for fruitful scholarship in this area.

Finally, but not least, I will like to thank my family for all of their support and encouragement throughout the course of my graduate studies.

A. Nolan Wilson
Friday, July 6th, 2012

ABSTRACT

Bioresponsive hydrogels are emerging with technological significance in targeted drug delivery, biosensors and regenerative medicine. Conferred with the ability to respond to specific biologically derived stimuli, the design challenge is in effectively linking the conferred biospecificity with an engineered response tailored to the needs of a particular application. Moreover, the fundamental phenomena governing the response must support an appropriate dynamic range and limit of detection. The design of these systems is inherently complicated due to the high interdependency of the governing phenomena that guide the sensing, transduction, and the actuation response of hydrogels. To investigate the dynamics of these materials, model systems may be used which seek to interrogate the system dynamics by uni-variable experimentation and limit confounding phenomena such as: polymer-solute interactions, polymer swelling dynamics and biomolecular reaction-diffusion concerns.

To this end, a model system, α-chymotrypsin (Cht) (a protease) and a cleavable peptide-chromogen (pro-drug) covalently incorporated into a hydrogel, was investigated to understand the mechanisms of covalent loading and release by enzymatic cleavage in bio-responsive delivery systems. Using EDC and Sulfo-NHS, terminal carboxyl groups of N-succinyl-Ala-Ala-Pro-Phe p-nitroanilide, a cleavable chromogen, were conjugated to primary amines of a hydrated poly(HEMA)-based hydrogel. Hydrogel discs were incubated in buffered Cht causing enzyme-mediated cleavage of the peptide and concomitant release of the chromophore for monitoring. To investigate substrate loading and the effects of hydrogel morphology on the system, the concentration of the amino

groups (5, 10, 20, and 30 mol%) and the cross-linked density (1, 5, 7, 9 and 12 mol%) were independently varied. Loading-Release Efficiency of the chromogen was shown to exhibit a positive relation to increasing amino groups (AEMA). The release rates demonstrated a negative relation to increasing cross-linked density attributed to decreasing void fractions and increasing tortuosities. The diffusion coefficient of Cht, $D_{0,Cht}$, was determined to be $6.9 \pm 0.5 \times 10^{-7}$ cm^2 s^{-1}, and the range of D_{eff} of Cht for 1 to 12 mol% TEGDA was determined to 6.9×10^{-8} to $0.1 \times 10^{-8} cm^2$ s^{-1}. We show how these parameters may be optimized and used to achieve programmed release rates in engineered bio-responsive systems.

The field of bioresponsive hydrogels is continuing to expand as the need for such materials persists. Future work will enable more control over the loading and release of therapeutic and diagnostic moieties. Continued research regarding in enzymatically actuated hydrogels will involve pre-polymerization loading methodologies; *in silico* diffusion-reaction multiphysics modeling; enzyme actuated degradation of the polymer; and substation of various mediating enzyme, cleavable peptides, and release molecules.

TABLE OF CONTENTS

Page

LIST OF FIGURES

LIST OF TABLES

Page

CHAPTER 1: BIORESPONSIVE HYDROGELS

1.1. Introduction

Biologically responsive (bioresponsive) hydrogels are a progressive iteration on stimuli responsive hydrogels wherein the response of the hydrogel is mediated by a biological recognition reaction. Hydrogel responses include, among others; swelling or collapsing, degradation or erosion, mechanical deformation, optical density variations, or electrokinetic variations [1]. Bio-responsive hydrogels link hydrogel responses to the innate specificity of bio-recognition reactions, and they are designed to elicit a predicted response when subjected to a biological agent [2]. Biological agents used to trigger engineered responses may be biomolecules like glucose [3], large macromolecules like chymotrypsin [4], or even whole cells, such as vascular endothelial cells [5, 6]. The response may be binary, as in presence or absence of the biological agent at a particular threshold limit, or it may be scalable with the chemical potential or activity of the biological agent [7-9]. Highly-specific recognition creates many opportunities for design of applications wherein a response will only occur when certain criteria have been met. This creates a "smart" material because it is cognizant of surrounding agents and can remain in stasis or become dynamic depending on changes in the surrounding environment [10, 11]. Bioresponsive hydrogels may share features with but are distinguished from biomimetic hydrogels that contain elements of chemistry, structure, architecture, morphology and materials properties intended to mimic local biological properties and from bioactive hydrogels that contain elements intended to participate within known biochemical pathways.

The utility of bioresponsive hydrogels is vividly apparent in their applications. These hydrogels have been used in tissue engineering [12, 13], in mediated drug delivery [14-16], and biosensing applications [17-19]. In tissue engineering, bioresponsive hydrogels have been used as biomimetic matrices, which promote cellular proliferation but also biodegrade over time . In drug delivery, it is commonly desired to deliver a drug in specified doses to a specific site, organ, or biological system [20-22]. Bio-responsive hydrogels are capable of location specific delivery because they are able to release the therapeutic drug payload when they are triggered by biologically derived, site-specific stimuli [23]. In sensor applications, bioresponsive hydrogels can produce a measurable response when a specific analyte of biological origin is present [24]

Although bioresponsive hydrogels have many potential applications and advantages, the engineering of these materials is often difficult due to the need for considerable molecular and architectural design; the biologically imposed constraints in conditions of materials processing; the complex interactions between the hydrogel matrix, the conferring bioactive species, the targeted biological agent, and the solvent (usually water) during performance. Successful design requires approaches that include multiple length scale theoretical and experimental modeling. Theoretical modeling of the bioresponsive hydrogels is advantageous as generalized models can be broadly applied; however, this approach requires detailed understanding of the interdependence of governing phenomena over multiple length scales [25-27] Conversely, empirical modeling can yield simple mathematical relations established from analysis of

experimental data, but careful considerations must accompany extrapolation of such empirical models to other systems or beyond the experimentally probed regimes [28, 29].

1.2. Fundamental Phenomena Effects Response

1.2.1. Biological Event, Transduction-Signal Creation, and Response

Before the governing phenomena and design considerations for bioresponsive hydrogels are addressed, the general mechanism for which a biological agent creates a response within a hydrogel will first be presented and discussed. The overarching platform technology may be considered as arising from the first three-steps illustrated in the process flow diagram of Figure 1.

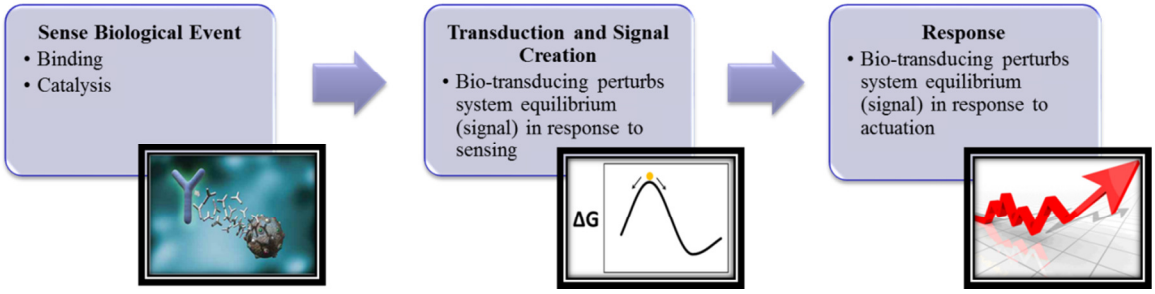

Figure 1: Information flow scheme of bio-responsive hydrogels.

First, a targeted biological agent comes into contact with the hydrogel and is "sensed" by a biorecognition species within the hydrogel; the species being specific to that agent. Bioactive species can be biomacromolecules like enzymes, antibodies, nucleic acids, or any native or synthetic biomimetic variants of the foregoing [30-33], or small molecules such as metabolites or peptides [34, 35]. The second step is transduction of the sensed agent into a perturbation of the thermodynamic equilibrium of the bioresponsive hydrogel system. One example would be where a substrate (targeted

biological agent) diffuses into a bioresponsive hydrogel conferred with the specificity of an immobilized enzyme which then catalyzes the conversion of that substrate to a product. The enzymatic reaction is forced away from equilibrium by a change in the chemical potential of the substrate that manifests a change in the chemical potential of the product. In bioresponsive hydrogels this perturbation is considered the signal which then elicits a response [1]. To establish a response, the hydrogel system must move to a new thermodynamic equilibrium based on the newly transduced conditions. For the case of the enzyme, this would be the chemical potential of the substrate motivated by catalysis of the substrate to product which will continue until all substrate is consumed or until the reaction reaches chemical equilibrium. The change in chemical potential of the product may elicit a collapse or swelling of the hydrogel. In this way, the chemical potential of a targeted agent is linked via a biorecognition reaction to a response of the hydrogel. An additional step, Step 4, an integrated control loop, is also illustrated in Figure 1 and discussed in the subsequent section. For example, the appearance of the product may induce a collapse of the hydrogel which reduces the diffusivity of the substrate into the hydrogel; in which case the chemical potential of the substrate will have a self-limiting effect on the response of the hydrogel.

1.2.2. Phenomena Governing Responses

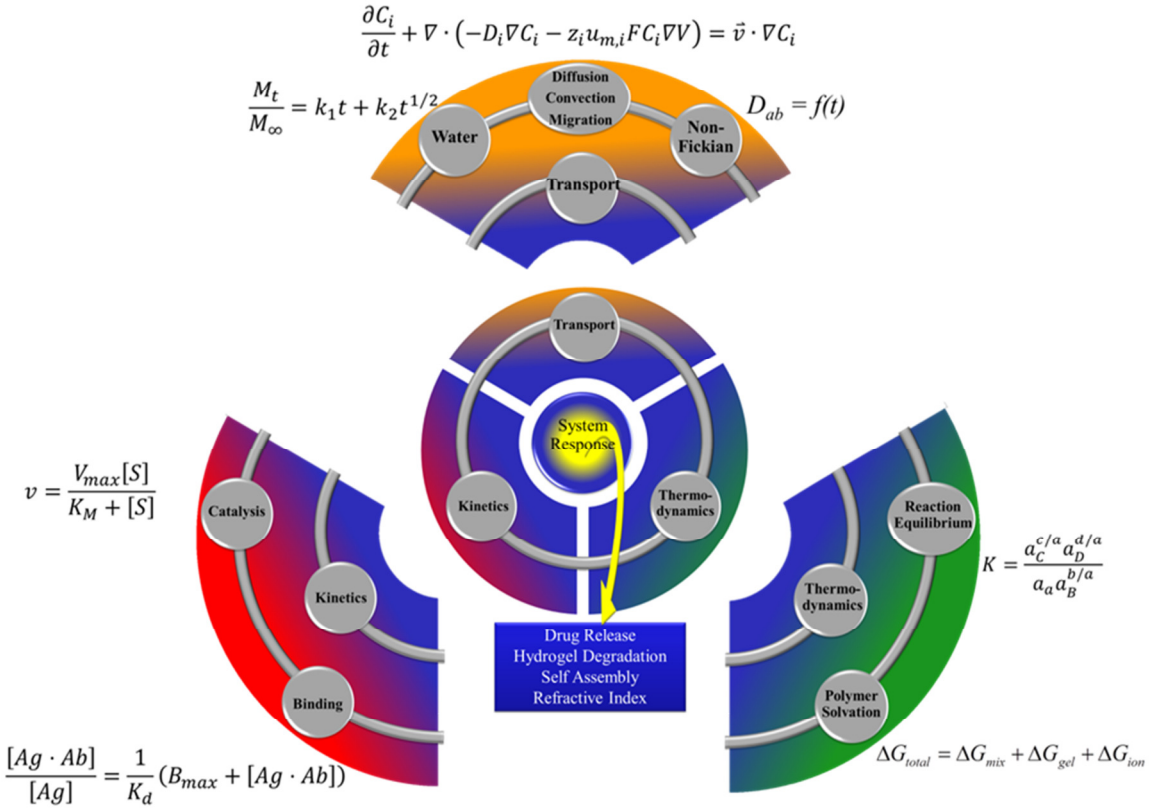

Figure 2: Interdependency of fundamental phenomena in bioresponsive hydrogels.

Bioresponsive hydrogels display a high degree of interdependency between response reaction kinetics, associated mass transport, and the kinetics and thermodynamics of the response phenomena, usually swelling or deswelling. This interdependency is useful because it allows for a wide range of ways to sense, transduce, and respond; however, it also necessitates a comprehensive understanding of the system because of the dynamic nature of interdependent phenomena. Figure 2 shows the dominant governing phenomena and associated governing equations and schematically traces through the interdependency of these phenomena in bioresponsive hydrogels. To

understand the dynamics of bioresponsive hydrogels, the three governing phenomena will be analyzed separately, and then their interdependencies will be considered.

1.2.2.1. Governing Phenomena – Reaction Kinetics

For bioresponsive hydrogels two widely used sensing mechanisms are enzymatic catalysis and receptor-ligand binding[2]. The fundamental equations commonly used to describe these reactions are Michales-Menten and Scatchard equations, respectively. The kinetics of these reactions are the limiting case for all other processes in the response. If all other steps in the process occurred instantaneously, which is rarely the case, the maximum rate for which the bio-responsive hydrogel could respond would be the maximum rate of the catalytic or binding reaction**.**

Although both enzymatic and binding reactions are well studied, the kinetics of these reactions can be modified by association with the hydrogel. In some systems the enzyme or receptor may be covalently immobilized. This immobilization may cause inactivation due to non-specific absorption or protein denaturation [36, 37]. In other immobilization techniques the bio-macromolecule may be entrapped within the hydrogel. This also may change the kinetics because the bio-macromolecule activity may be reduced during immobilization [38]. While immobilization can reduce activity, it often increases stability over time and tradeoffs between the two should be considered in design. For bio-responsive hydrogels, the kinetics of bio-macromolecules inside the hydrogel should be studied in conjunction with the kinetics of these molecules in solution to ascertain the effects the hydrogel environment has on the bio-macromolecule.

For the case of any reaction that is not zero order, the effects that mass transport limitations or thermodynamic changes in the hydrogel may have on the reaction kinetics of the bio-macromolecule should be considered. Mass transport may affect the kinetics because it can reduce the amount of substrate available for reaction [36]. The thermodynamics of the hydrogel will govern the hydration and swelling of the gel, and because the activity of bio-macromolecules can be affected by the amount of water present, the thermodynamics can directly affect the kinetics of the biomolecular reaction [39].

1.2.2.2. Governing Phenomena – Mass Transport

Transport within bio-responsive hydrogels directly affects the time dependent response of these materials by changing the local availability of bioactive moieties. The rate of transport in and out of a hydrogel can be influenced by diffusion, convection, or electrical gradients and is described by the Nernst-Plank equation [40-44].

Diffusive transport, the most prevalent mode of transport in hydrogels, occurs via the water-filled pores/voids and fundamentally is driven by chemical potential gradients; however, in practice concentration gradients are used. Ficks first and second law are the basis for diffusive transport. Improvement to Ficks law has required diffusion coefficients which depend on concentration or polymer properties [45]. These models include the free volume theory, hydrodynamic theory, and obstruction theory [46]. Free volume theory considers diffusion as a process which solute molecules hop into discrete voids spaces created by the dynamic redistribution of solvent molecules and assumes the

redistribution can occur with no change in free energy [47]. Hydrodynamic theory is based on Stokes-Einstein equation for solute diffusivity, wherein the solute is treated as a hard sphere. Mathematically the model is the ratio of the thermal energy divided by a frictional drag coefficient [48]. Obstruction theories treat the polymer as impenetrable chains effecting tortuosity of the diffusion path. Improvements to this theory include models using distributive probability functions describing the probability of a solute passing through a space in the polymer mesh [49, 50]. Application of transport models to bio-responsive hydrogels will depend on solute-polymer interactions and polymer morphology. Table 1 lists models which can be applied to various morphologies.

Table 1: Diffusive transport theories as they apply to hydrogel morphology.

Theory	**Hydrogel Morphology**	**Equation**		**Ref**
Free Volume	Porous	$D_{ip} = \frac{(\lambda^*)^2 v}{6}$	(1)	[46, 51, 52]
Free Volume	Nonporous, Highly Swollen	$\frac{D_{ip}}{D_{iw}} = k_1\left(\frac{\bar{M}_c - \bar{M}_c^*}{\bar{M}_n - \bar{M}_c^*}\right)\exp\left(\frac{-k_2 r_s^2}{Q-1}\right)$	(2)	[46, 52, 53]
Hydrodynamic	Micro-Porous	$\frac{D_{ip}}{D_b} = (1-\lambda)^2(1+\alpha\lambda+\beta\lambda^3+\gamma\lambda^5)$	(3)	[46, 52, 54]
Obstruction	Porous	$D_{ip} = D_{iw}K_pK_r\frac{\varepsilon}{\tau}$	(4)	[46, 52, 55]

Where D_{ip} is the diffusion coefficient of species i in the polymer matrix; D_b is the diffusion coefficient of the solute through the bulk; D_{iw} diffusion coefficient of species i

in the solvent; λ^* is the diffusional jump length of the solute; υ is the jump frequency; $\bar{M}_c$ is the average molecular weight between crosslinks; $\bar{M}_n$ is the average molecular weight of the polymer without crosslinks; $\bar{M}_c^*$ is the critical molecular weight between crosslinks; λ is the ratio of the solute radius to the average pore radius; α, β, and γ are constant dependent on the system; K_p is the partitioning coefficient; and K_r is the fractional reduction in diffusivity as the solute diameter approaches the pore diameter.

A separate but equally important consideration to modeling solute transport in hydrogels is the constitutive equation which will be applied to match the release profile. Many approaches have been taken based on empirical and semi-empirical models. These models offer relatively high predictability of solute transport without requiring intricate knowledge of the polymer-solute interactions and mathematically are relatively simple. Table 2 lists several of these models.

Table 2: Empirical and Semi-empirical models for solute diffusion in hydrogels.

Model	Equation		Special Constraints	Ref
Hixson Crowell Cube Root	$W_0^{1/3} - W_t^{1/3} = kt$	(6)		[56]
Korsemeyer-Peppas	$\frac{M_t}{M_\infty} = kt^n$	(7)		[56]
First-Order	$\ln\left(\frac{M_0}{M_t}\right) = kt$	(8)		[56]
Zero-Order Kinetic Model	$M_0 - M_t = kt$	(9)		[56]
Peppas Anomalous Transport	$\frac{M_t}{M_\infty} = k_1 t + k_2 t^{1/2}$	(10)	$n > 0.5$	[57]

Where k, k_1, k_2, n, and A are constants dependent on the system; M_i is the solute concentration at a given time, t; W_i is the weight of the solute at a given time, t; D is the diffusivity coefficient; and L is slab thickness.

Equation (7) allows solute transport to be determined as less Fickian, Fickian, or anomalous transport based on the experimentally determined value of n: $n < ½$ in less Fickian, $n = ½$ in Fickian, and $n > ½$ for anomalous transport. Fickian or less Fickian transport indicates water penetration rate is less than the polymer chain relaxation rate. Anomalous transport indicates water penetration rate occurs faster than the hydrogel relaxation rate. Constants k_1 and k_2 in Equation (10) describe the rate of relaxation controlled transport and the rate of diffusion controlled transport [58], respectively. In the application of these models it is common to utilize the model which yields the greatest least-squared regression is used to determine the most applicable model.

The need for more accurate predictions based on system parameters, specifically geometry and solubility state, in diffusion limited drug delivery systems has led to the development of explicitly derived release equations. Equations for slab, cylindrical, and spherical geometries have been developed for non-constant activity release sources, where the drug is completely separate from the releasing membrane (shell-core-structure) and below its solubility limit; constant activity release sources, where the drug is completely separate from the releasing membrane (shell-core-structure) but above its solubility limit; monolithic release solutions, where the drug is homogenously distributed within the releasing material and below its solubility limit; and monolithic release dispersions, where the drug is homogenously distributed within the releasing material but above its solubility limit [59]. The derived equations and simplified approximations are presented in Table 3. For the complete, explicitly derived equations, detailed summary of the applications, assumptions, and special cases, such as lag-time or burst phase, the reader is directed to the literature [45, 59].

Table 3: Explicitly derived equations and time approximations for diffusive transport of species from hydrogel [59].

Source Type	Geometry	Equation		Special Constraints
Non-Constant Activity Source	Slab	$\frac{M_t}{M_\infty} = 1 - \exp\left(-\frac{ADKt}{VL}\right)$	(11)	
	Cylinder	$\frac{M_t}{M_\infty} = 1 - \exp\left(-\frac{(R_i H + R_0 H + 2R_i R_0)DKt}{R_i^2 H(R_0 - R_i)}\right)$	(12)	
	Sphere	$M_t = \frac{2\pi HDKC_s}{\ln(R_o/R_i)}t$	(13)	
Constant Activity Source	Slab	$M_t = \frac{ADKC_s}{L}t$	(14)	
	Cylinder	$M_t = \frac{4\pi DKC_s R_0 R_i}{R_0 - R_i}t$	(15)	
	Sphere	$M_t = \frac{2\pi HDKC_s}{\ln(R_o/R_i)}t$	(16)	
Monolithic Solution	Slab	$\frac{M_t}{M_\infty} = 4\left(\frac{Dt}{\pi L^2}\right)^{1/2}$	(17)	Early times $M_t/M_\infty \leq 0.6$
		$\frac{M_t}{M_\infty} = 1 - \frac{8}{\pi^2}\exp\left(-\frac{\pi^2 Dt}{L^2}\right)$	(18)	Late times $M_t/M_\infty \geq 0.4$
	Cylinder	$\frac{M_t}{M_\infty} = 4\left(\frac{Dt}{\pi R^2}\right)^{1/2} - \frac{Dt}{R^2}$	(19)	Early times $M_t/M_\infty \leq 0.6$
		$\frac{M_t}{M_\infty} = 1 - \frac{4}{2.405^2}\exp\left(-\frac{2.405^2 Dt}{R^2}\right)$	(20)	Late times $M_t/M_\infty \geq 0.4$
	Sphere	$\frac{M_t}{M_\infty} = 6\left(\frac{Dt}{\pi R^2}\right)^{1/2} - \frac{Dt}{R^2}$	(21)	Early times $M_t/M_\infty \leq 0.6$
		$\frac{M_t}{M_\infty} = 1 - \frac{6}{\pi^2}\exp\left(-\frac{\pi^2 Dt}{R^2}\right)$	(22)	Late times $M_t/M_\infty \geq 0.4$
Monolithic Dispersion	Slab	$M_t = A\sqrt{DC_s(2C_{ini} - C_s)t}$	(23)	
	Cylinder	$\frac{M_t}{M_\infty} - \frac{3}{2}\left[1 - \left(1 - \frac{M_t}{M_\infty}\right)^{2/3}\right] = -\frac{3DC_s}{R^2 C_{ini}}t$	(24)	
	Sphere	$\frac{M_t}{M_\infty} + \left(1 - \frac{M_t}{M_\infty}\right)\ln\left[1 - \frac{M_t}{M_\infty}\right] = \frac{4DC_s}{R^2 C_{int}}t$	(25)	

Where M_t and M_∞ is the cumulative amount of drug released at time t and ∞, respectively; A is the total surface area normal to the diffusive release path; D is the diffusion coefficient of the solute; K is the partitioning coefficient of the solute between the membrane and the reservoir; V is volume of the reservoir; L is the membrane thickness; R_i and R_0 are the inner and outer radius, respectively, of the cylinder or sphere membrane; H is the cylinder length; R is radius of the cylinder or sphere; C_s is drug solubility in the reservoir or wetted matrix for constant activity or monolithic dispersion source types, respectively; and C_{int} is the initial loading concentration.

Convective transport is caused by external velocity gradients or by equilibrium changes which cause water to move in or out of the hydrogel. In both cases, species solvated by water will be subject to convective transport. This type of transport is best exemplified by super-porous hydrogels (SPHs), hydrogels with pore sizes in the several hundred micrometer range; such SPHs rapidly imbibe water via capillary forces [60]. In addition to convective transport, transport due to electrical gradients is usually coupled with other thermodynamic phenomena such as: swelling, deswelling, or erosion [61]. The interaction of three potential fields, chemical, electrical and mechanical, must be considered when modeling transport within hydrogels. Wallmersperger et al., describes methodologies for modeling such systems [62].

Understanding transport in bioresponsive hydrogels empowers predictive coupling with kinetic and thermodynamic phenomena to engineer more complex systems. Various theoretical and empirical models can be used, but care must be taken in the

selection of the appropriate equations to accurately predict transport and its relation on other fundamental phenomena.

1.2.2.3. Governing Phenomena – Thermodynamics

Thermodynamic equilibrium plays a principal role in the design of bioresponsive hydrogels. While coupled mass transport and biorecognition reaction kinetics guide temporal processes, thermodynamics govern direction of change and final state of the system. Here, two thermodynamic phenomena, polymer solvation theory and chemical equilibrium theory, will be considered.

Polymer solvation theory originated with the lattice based Flory-Huggins (1942) theory which sums the free energy of mixing of network chain elements and solvent, ΔG_{mix}, electro-osmotic pressure within the network due to mobile couterions, ΔG_{ion}, and elastic retractile force of the polymer network, ΔG_{gel} [63-66], Equation (26), and its subsequent derivation results in Equation (27)

$$\Delta G_{mix} + \Delta G_{gel} + \Delta G_{ion} = -\left(\frac{\partial \Delta G}{\partial V}\right)_{T,n_i} = 0 \qquad (26)$$

$$\pi_{mix} = -\frac{RT}{V_1}[ln(1-v) + v + \chi v^2] \qquad (27)$$

Where V_1 is the molar volume of the solvent, π_{mix} is the osmotic pressure of the polymer solution, ν is the polymer volume fraction, and χ represents the change in the interaction energy upon the mixing of the polymer and solvent. Low values of χ is associated with high polymer-solvent intercations and low hydrophobic interactions, which are indicative

of highly hydrophilic polymers [67]. χ may be readily calculated for hydrogels using Equation (28) [68, 69].

$$\chi = -\frac{\ln(1-\phi_2)+\phi_2+\upsilon_e V_1\left(\phi_2^{\frac{1}{3}}-2\phi_2 f^{-1}\right)}{\phi_2^2} \qquad (28)$$

Where υ_e is the effective crosslink density, φ_2 is the polymer volume fraction, and f is the functionality of the crosslinker. Extensions of Flory-Huggins theory lead to models which predict lower critical solution temperature [70, 71], a critical parameter for temperature responsive hydrogel. Further modification of the theory by Peppas and Merrill accounts for hydrogels prepared in solvent, water, by considering the volume fraction density of chains during crosslinking in a neutral hydrogel and results in a relation to determine molecular weight between crosslinks $\bar{M}_c$ Equation (29) [72].

$$\frac{1}{\bar{M}_c} = \frac{2}{\bar{M}_n} - \frac{(\bar{\upsilon}/V_1)\left[\ln(1-\upsilon_{2,s})+\upsilon_{2,s}+\chi_1\upsilon_{2,s}^2\right]}{\upsilon_{2,r}\left[\left(\frac{\upsilon_{2,s}}{\upsilon_{2,r}}\right)^{1/3}-\left(\frac{\upsilon_{2,s}}{2\upsilon_{2,r}}\right)\right]} \qquad (29)$$

Where $\bar{M}_n$ is the molecular weight of the polymer chains absent of the crosslinking agent, $\bar{v}$ is the specific volume of the polymer, V_1 is the molar volume of the water, $\upsilon_{2,r}$ is the polymer volume fraction immediately after crosslinking (relaxed state), and $\upsilon_{2,s}$ is the polymer volume fraction in the swollen state. Determination of $\bar{M}_c$ allows for the calculation of the linear distance between adjacent crosslinks, ξ, which is considered the pore or mesh size. ξ provides valuable insight into polymer morphology and can be readily applied to transport models which predict diffusivity constants [50]. Calculation of ξ can be made by combination of Equations (29) and (30).

$$\xi = \upsilon_{2,s}^{-1/3}\left(\frac{2C_n\bar{M}_c}{M_r}\right)^{1/2} l \qquad (30)$$

Where C_n is the Flory characteristic ratio, M_r is the molecular weight of repeat unit, and l is the bond length along the polymer backbone. Determination of $\bar{M}_c$ can also be performed through mechanical methods relating applied stress or modulus to $\bar{M}_c$ by extentions of rubber elasticity theory [72, 73].

Cationic and anionic hydrogels are readily extended as bioresponsive hydrogels by the incorporation of enzymes which create localized changes in pH through catalysis subsequently changing the thermodynamic state of the polymer [74, 75]. They have also been used in applications where biological changes in pH actuate a response[76]. Swelling relations for cationic and anionic polymers prepared in the presence of solvent have been derived, Equations (31) and (32), respectively.

$$\frac{V_1}{4I}\left(\frac{v_{2,s}^2}{\bar{v}}\right)\left(\frac{K_b}{10^{14-pH}-K_a}\right)^2 = \left[\ln\left(1-v_{2,s}\right)+v_{2,s}+\chi_1 v_{2,s}^2\right]+\left(\frac{V_1}{\bar{v}\bar{M}_c}\right)\left(1-\frac{2\bar{M}_c}{\bar{M}_n}\right)v_{2,r}\left[\left(\frac{v_{2,s}}{v_{2,r}}\right)^{1/3}-\left(\frac{v_{2,r}}{v_{2,r}}\right)\right] \qquad (31)$$

$$\frac{V_1}{4I}\left(\frac{v_{2,s}^2}{\bar{v}}\right)\left(\frac{K_a}{10^{-pH}-K_a}\right)^2 = \left[\ln\left(1-v_{2,s}\right)+v_{2,s}+\chi_1 v_{2,s}^2\right]+\left(\frac{V_1}{\bar{v}\bar{M}_c}\right)\left(1-\frac{2\bar{M}_c}{\bar{M}_n}\right)v_{2,r}\left[\left(\frac{v_{2,s}}{v_{2,r}}\right)^{1/3}-\left(\frac{v_{2,r}}{v_{2,r}}\right)\right] \qquad (32)$$

Where I is ionic strength and K_a and K_b are the acid and base dissociation constants, respectively [52].

Reaction equilibrium in bioresponsive hydrogels can be determined by fundamental Equations (33) and (34) [77]. Generally, reaction equilibrium can be considered less important than reaction kinetics. In catalyzed reactions, the reaction occurs quickly relative to other phenomena occurring in the system, e.g. polymer swelling or mass transport. Therefore, pseudo equilibrium is usually a reasonable

assumption for the catalyzed reaction unless the system is designed to negate rate limiting phenomena. In binding reactions, the equilibrium lies far to the right so it can be assumed that all free species will be bound until the binding sites become saturated. While these assumptions are generally true, reaction equilibrium has been leveraged to engineer novel systems. In one example, an enzyme which normally hydrolyzes peptide bonds is used in the self-assembly of nanofibrous peptide structures by reversing the normal reaction direction [78].

$$A + \frac{b}{a}B \rightleftharpoons \frac{c}{a}C + \frac{d}{a}D \tag{33}$$

$$K = \frac{a_C^{c/a} a_D^{d/a}}{a_a a_B^{b/a}} \tag{34}$$

1.3. Response Types

1.3.1 Swelling or Collapse - pH and Ionic Actuation

Hydrogels are 3D cross linked networks of highly hydrophilic monomer containing moieties such as ethers, thiols or hydroxyls and ionizable groups such as carboxyls and amines. The latter groups have individual pKa values which, depending on monomer composition and dissociation strength, will produce a net charge on the hydrogel. Net charge neutrality is maintained by balancing the hydrogel charge with counterions drawn from the solution. The increased concentration of ions leads to an electroosmotic pressure as well as a space charge layer that extends into the diffusion layer in solution. A hydrogel in solution will thus reach an equilibrium swelling point where the osmotic pressure force, which drives water into the hydrogel, is balanced by

the mechanical retractile forces of the chemical bonds holding the matrix together. This balancing of osmotic and mechanical forces in a hydrogel matrix is similar to the deformation of a spring to which a force is applied [79-81].

Changes in internal charge balance actuate swelling or collapse of hydrogels. Changes in solution pH or ion concentration (dielectric constant) can force the solution and hydrogel away from equilibrium. To restore equilibrium, protons or other ions will diffuse into or out of the hydrogel restoring net charge neutrality. Mechano-osmotic equilibrium is reestablished by the transport of water into or out of the hydrogel. This process has been modeled using a FEM approaches which combines transport, Equation (35), electrostatics, Equations (36-37), and mechanical deformation, Equations (38-41) [82, 83].

$$\frac{\partial C_i}{\partial t} + \nabla \cdot \left(-D_{eff,i}\nabla C_i - z_i u_{m,i} F C_i \nabla V\right) = R_i \qquad (35)$$

Where Equation (35) is the Nernst-Planck equation with *C* as concentration of species *i*, D_{eff} is the effective diffusivity, *z* is the ion valence, u_m is the ion mobility, *F* is Faraday's constant, *V* is potential, and *R* is a reaction term.

$$\nabla \cdot (-\epsilon_0 \epsilon_r \nabla V) = F(z_{H^+} C_{H^+} + z_{A^-} C_{A^-}) \qquad (36)$$

$$\left(\frac{C_{k+}}{C_{k+}^0}\right)^{\frac{1}{|z_{k+}|}} = \left(\frac{C_{k-}^0}{C_{k-}}\right)^{\frac{1}{|z_{k+}|}} = \lambda \qquad (37)$$

Electrostatic migration can be coupled to transport by Equation (36) which combines the Helmholtz and Gauss laws relating charge density to potential. Where ε_0 and ε_r are the vacuum and relative permittivities of the ion, respectively. Alternatively, Donnan

potential has been used to calculate ion concentrations; where C_{k+}, C_{k+}^{0} and positive ion concentrations inside and outside the gel and C_{k-} and C_{k-}^{0} are negative ion concentrations inside and outside the gel, respectively. Donnan potential assumes the partitioning ratio, λ, to be constant and Equation (37) is not used contribute to temporal electro-migratory transport. This approach can be taken to reduce computational expense [84].

$$\sigma_{ij} = E_{ijkl}\left(u_{k,l} - (\varepsilon_{\pi})_{kl}\right) \tag{38}$$

$$\epsilon_{\pi} = k(\Delta\pi - \Delta\pi_0) \tag{39}$$

$$\Delta\pi = RT\sum_{\alpha=1}^{N_f}\left(C_{\alpha} - C_{\alpha}^{ref}\right) \tag{40}$$

$$f\frac{du_i}{dt} = \sigma_{ij,j} + \rho b_i \tag{41}$$

Mechanical stress-strain deformations have been coupled temporal concentration changes via osmotic pressure; where σ is the stress tensor; E is the elasticity tensor; u is the geometric strain; ε_{π} is the swelling strain; k is the swelling coefficient; π and π_0 are the osmotic and initial differential osmotic pressures, respectively; R is the ideal gas constant; T is temperature; C_{α} and C_{α}^{ref} are the concentrations and reference concentration at the gel-solution boundary, respectively; f is the mechanical damping parameter; ρ is the mass density; and b is the volume forces.

In one such model the reversible swelling and collapse of a pH responsive chitosan hydrogel was explored through FEM and compared to experimental results for a pH range between 5.0 and 8.5, Figure 3 [84, 85]. While models for swelling and collapse have been successfully demonstrated experimentally, using a FEM approach to model pH

or ion actuated drug release is largely unexplored in the literature and is an ongoing area of research.

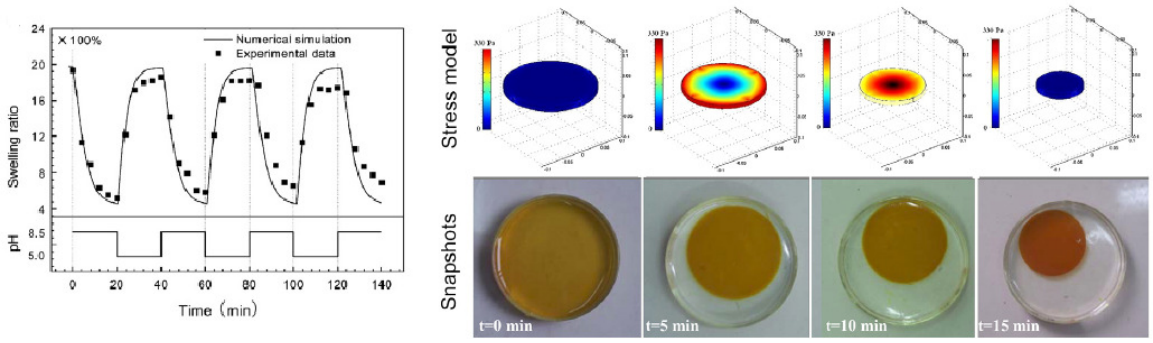

Figure 3: Comparison of experimental to theoretical results for a pH responsive chitosan hydrogel from a FEM approach.

Others have used bioresponsive hydrogels in biosensors and as stimuli responsive drug delivery vehicles [76]. In one construct, a pH responsive polymer, poly(2-vinylpyridine-*co*-divinylbenzene), was conjugated to gold nanoparticles containing magnetic iron oxide (IONPs) and fluorescent CDSe/ZnS quantum dots (QD). This construct allowed for a multi-responsive system wherein the pH responsive polymer enabled size control, the IONPs enabled manipulation via magnetic fields, and the QDs enabled fluorescence detection [86]. In other work, the activity of molecularly imprinted polymers (MIPs) has been tuned via the addition of a pH responsive polymer to the construct. MIPs designed to mimic the active sites of enzymes are typically more stable than their biological equivalents but often lack the binding. A MIP which mimics the catalytic ability of a peroxidase was conjugated with pH responsive polymers to form nanospheres wherein the catalytic ability of the nanospheres was shown to be a function of pH and had an optimum pH of 8.3 [87].

1.3.2 Erosion and Degradation

Another response that has been leveraged in the application of bioresponsive hydrogels is the degradation or erosion of the polymer matrix in response to a biomediated stimulus. For this discussion degradation will be considered the breakdown of the polymer matrix into monomeric constituents which were originally polymerized to create the matrix, and erosion is breakdown of the polymer matrix into smaller oligomeric chains wherein some polymeric constituents remain intact.

Eroding hydrogels have found wide acceptance in tissue engineering and drug delivery applications. At the root of the erosion process is the hydrolysis of a labile bond that is part of the hydrogel backbone and/or crosslinks. Commonly, this is the hydrolysis of an ester bond, as in poly(lactic acid) (PLA) or poly(lactic-co-glycolic acid) (PLGA); however, the hydrolysis of an anhydride or anhydride-*co*-imide bond, as in poly(sebacic acid) or poly-[trimellitylimidoglycinr-*co*-bis (carboxyphenoxy) hexane)], has been demonstrated [88-90]. Erosion rates in thermoplastics can be controlled by chemical composition and processing methodologies which can alter crystalline and amorphous regions in the material. Additionally, the polymer can be surface or bulk eroding where the water penetration rate is slower than the erosion rate or vice versa. Eroding hydrogels are becoming more widely used as their mechanical integrity is improved, tuneability of their thermal responsiveness is more easily accomplished, processability difficulties are addressed, and polymers with cytotoxic pH byproducts from erosion have been replaced by polymers with neutral pH byproducts. Specifically, the poly(ortho ester) IV family has addressed most of these problems and is being developed commercially [88, 91].

Alternative to erosion, degradation involves breakdown of the polymer matrix into monomer and smaller oligomeric chains. Nonspecific degradation can occur via a hydrolytically unstable bond within the matrix or may occur enzymatically wherein esterases or peptidases cleave ester or amide bonds, respectively [11, 92]. Enzymatically triggered degradation in drug delivery and tissue engineering allows for targeted, controlled degradation of the polymer. The triggered degradation of the polymer matrix is advantageous because the matrix can remain in its native state until it is exposed to a specific enzyme. Degradation rates can be controlled by varying concentrations of the enzymatically cleavable crosslinking substrate, altering the sequence to increase or decrease its enzymatic affinity or reactivity, or altering the morphology of the hydrogel matrix effecting enzyme access [93, 94]. In one construct, an *in situ* gelating, enzyme degradable hydrogel was synthesized for soft tissue augmentation wherein the gel could be injected post-surgery to act as a synthetic scaffold for cellular proliferation. This gel was able to polymerize without the use of potentially cytotoxic free-radical initiators, a major concern for injectable hydrogels. Additionally, a cellular adhesion peptide was attached as a pendant group to promote receptor mediated cellular attachment. A collagenase cleavable peptide was integrated into the hydrogel backbone to support enzyme mediated degradation, Figure 4 [95]. In another example, a hydrogel matrix was synthesized that was susceptible to degradation by matrix metalloproteases (MMPs). The dextran based hydrogel was cross-linked with a MMP-cleavable peptide motif via maleimide functional groups [31]. MMP mediated degradation of hydrogel matrices is an

ongoing area of interest as these enzymes are an integral part of tissue reconstruction [96].

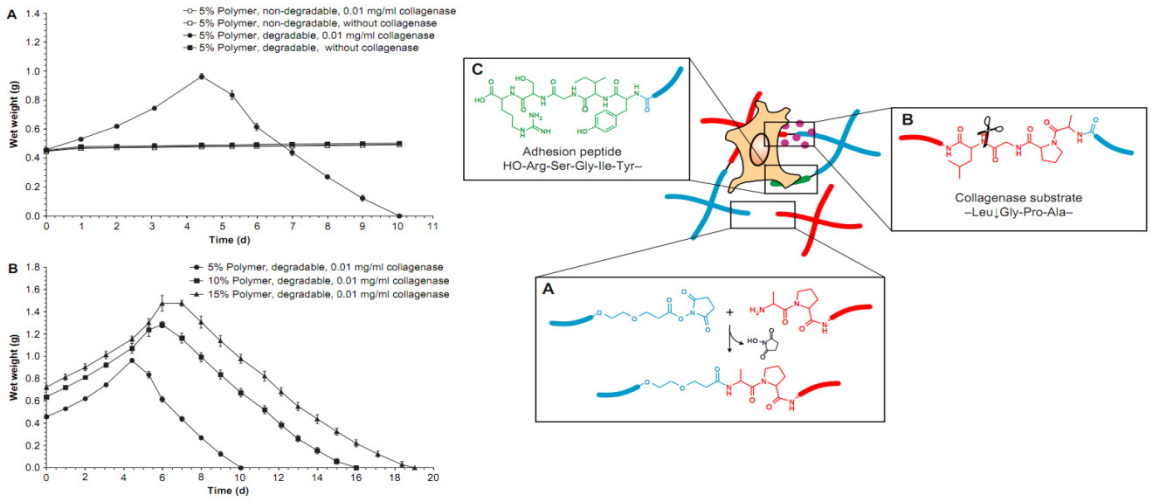

Figure 4: A bioresponsive hydrogel which gels in situ and degrades when exposed to collagenase [95].

1.3.3 Release

Bioresponsive hydrogels have been used extensively as vehicles for the delivery of therapeutic molecules. It is common to use a biological stimuli such as pH [97], redox potential [98], activity of biomacromolecules [11] or concentration of metabolites [34] to trigger release from the hydrogel. Other stimuli such as temperature [99], ultrasound [100], light [101], and magnetic fields [102] have been used to trigger release of drugs; however, these are considered environmental stimuli and therefore are outside the scope of this discussion. Using bioresponsive hydrogels as triggered release vehicles allows for tighter control over the amount of drug being delivered, the rate at which it is administers, and can reduce unwanted side effects to ancillary systems because the drug is localized only to desired regions and release is motivated by the activity of a biomarker. The mechanism for release can occur through physical changes to the

hydrogel matrix such as erosion, degradation, swelling, collapse, or through enzymatic cleavage.

An application of controlled release was demonstrated through the creation of a hydrogel-enzyme construct which mimicked the role of the pancreas by releasing insulin upon exposure to glucose. The hydrogel, possessing a pH responsive pendant amine, dimethylaminoethyl methacrylate (DMAEMA, pKa = 7.5), was co-loaded with glucose oxidase (GOx) and insulin. Upon exposure to glucose, GOx oxidized the glucose creating hydrogen peroxide and gluconic acid. The gluconic acid reduced the local pH within the hydrogel causing protonation of the DMAEMA and promoting electro-osmotic swelling thereby increasing the effective diffusivity of insulin within the matrix and promoting its release. The authors were also able to demonstrate zero-order release behavior by non-uniform loading of insulin within the hydrogel matrix [3]. In other work, the mechanism of loading through covalent attachment and the control of release rate were explored. The authors stoichiometrically controlled the loading of a peptide-linked chromogen by varying the mole fraction of the pendant, conjugatable amine group of co-polymerized aminoethylmethacrylate (AMEA). Release of the chromophore was mediated by exposure to chymotrypsin which cleaved the covalently attached peptide. The release rate was controlled by changing the cross-linker concentration, and in effect, the apparent diffusivity of chymotrypsin [103].

1.3.4 Mechanical

1.3.4.1 Gelation

In situ gelation has become an emerging trend in the application and research of bioresponsive hydrogels. Hydrogels that can cross-link *in vivo* following injection are desirable because they can be implanted as solutions using a syringe and so they can negotiate close-fitting tissue-to-gel contact in comparison to precast hydrogels. Physically crosslinking and photo-crosslinking approaches have been demonstrated; however, they have drawbacks such as low mechanical strength and the need for cytotoxic photo-initiators, respectively. An alternative approach being explored is enzyme mediated cross-linking of hydrogels [30, 104]. The gelation of such hydrogels occurs by the linking of pendant groups through enzymatic catalysis. *In situ* cross-linking of phenol moieties which were attached to a dextran-tyramine (Dex-TA) based hydrogel has been demonstrated. The cross-linking was mediated by horseradish peroxidase (HRP) and degradation of the hydrogel was realized through hydrolysis of the ester bonds. Gelation rate was shown to be dependent on HRP/TA ratio [30]. For further discussion of *in situ* hydrogel formation the reader is directed to Van Tomme [105].

1.3.4.2 Shape Transformation

The shape of a hydrogel construct is known to effect drug carrier performance [106]. Engineering the ability to biologically trigger a shape change of a bioresponsive hydrogel is of growing interest. As an example, spherical and elliptical hydrogels experience different hydrodynamic forces as they move through the vasculature.

Additionally, elliptical hydrogels have been shown to avoid phagocytosis more readily than spherical hydrogels. While elliptical hydrogels are not phagocytosed as readily, they also do not undergo endocytosis at the targeted cell as readily as spherical gels. This makes it desirable to have an elliptical hydrogel in the vasculature, and then have a spherical hydrogel near the delivery site [107]. To this end, a bioresponsive hydrogel which can change shape upon a tissue specific stimulus are being explored. In one construct a shape transformational hydrogel was created which changes from elliptical to spherical orientation in response to pH, temperature and an analyte. The shape change is driven by the balance of interfacial tension and polymer viscosity, Figure 5 [108].

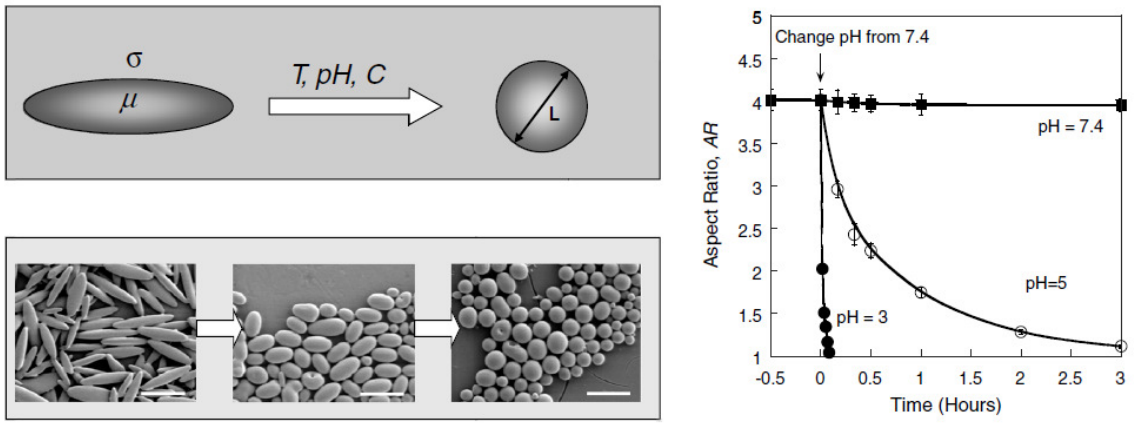

Figure 5: Temperature, pH, and chemically responsive hydrogel which changes shape from an elliptical to a spherical configuration based on environmental conditions [108].

1.3.5 Optical

Bioresponsive hydrogels that exhibit an optical response to a stimulus are gaining traction as a viable platform for biodetection and biosensing. The mechanism for detection or sensing may result from swelling or collapse of the hydrogel matrix that changes the shape of a lens [109], changes the refractive index[110], gelation [111],

turbidity, or induces a change in absorption or an emission [112]. In each case the change in the hydrogel matrix causes a detectable or measurable optical response. Additionally, chromophores or fluorophores may be released pursuant to binding or become activated by catalysis [1, 4, 113]. Responses can be visible by the naked eye or may require measurements of absorbance or emission at specific wavelengths [17, 111]. In a more recently developed system, thioglycolic-acid-capped quantum dots (CdSe QDs) were covalently attached to an acrylamide based hydrogel microspheres that were cross-linked with DNA motifs. When exposed to the complimentary strand of targeted DNA, the binding of the DNA strands resulted in hydrogel collapse due to the uptake of counterions. The collapsing event resulted in a blue shift in the Bragg diffraction peak. This system proved to be highly sensitive, down to 1 nM, and could differentiate DNA sequences that differed by one base pair, Figure 6 [114].

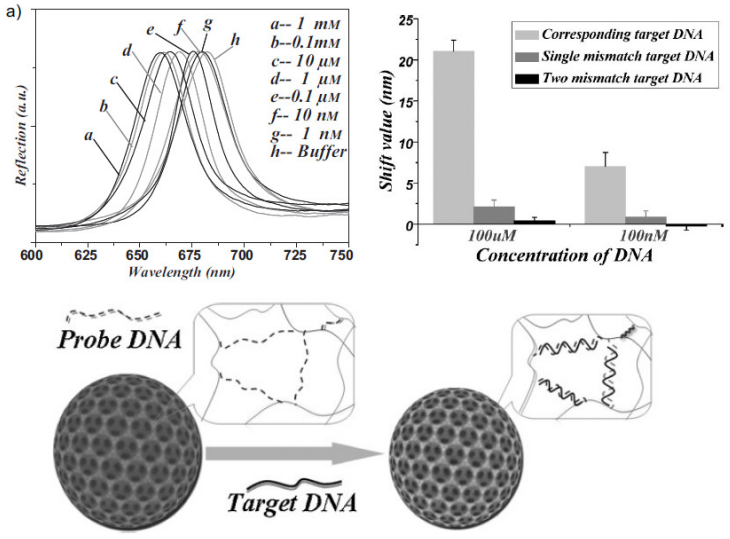

Figure 6: DNA sensing bioresponsive, quantum dot loaded hydrogel which elicits a shift in its peak absorbance upon exposure to the complimentary target DNA [114].

1.3.6 Electrochemical

Due to their high biocompatibility, hydrogels have been widely used in biosensors, both as an interface between tissue and electrode and also as a host for bioactive molecules[115]. By incorporating oxidoreductase enzymes into the polymer matrix, the biospecificity of the enzyme is conferred to the transducer and the enzyme stabilized in a hydrated 3-D milieu[116]. In amperometric, biosensors the electrodes act as an eventual source or sink for the electrons being transferred by the enzyme. Biosensors which measure analyte concentrations have been designed based on other electrical properties such as potential or impedance [18]. To increase sensitivity, reduce interfacial impedance, reduce interference from endogenous and exogenous species, and improve biocompatibility, electroconductive polymers such as polyaniline, polythiophene and polypyrrole, have been synthesized into the voids of the hydrogel matrix [18]. The resulting electroconductive polymer hydrogel composites also show the potential for programmed release of loaded drugs under modest voltage stimulation. Another approach to facilitate electron transfer in biosensors is the conjugation of the redox enzyme to single-walled carbon nanotubes (SWNT). Enzyme-SWNT conjugates have been shown to increase the peak current; additionally, graphene based biosensors are also being developed based on similar principles[117, 118] and may be incorporated into hydrogels. These composite materials add new response modes to the bioresponsive hydrogels.

1.4. Remarks and Conclusions

Bioresponsive hydrogels are increasingly being studied because they are highly biospecific, and they exhibit controlled response readily co-joined with biomolecular recognition. Moreover, there are many technological opportunities in targeted drug delivery, biosensors and regenerative medicine that motivate continued energetic pursuit of devices based on bioresponsive hydrogels. The design challenge is in effectively linking the conferred biospecificity with an engineered response tailored to the needs of a particular application. Moreover, the fundamental phenomena governing the response must support an appropriate dynamic range and limit of detection. The design of these systems is inherently complicated due to the high interdependency of the governing phenomena that guide the sensing, transduction, and the actuation response of hydrogels. While the dynamics between these phenomena are continually being investigated, bioresponsive hydrogels can still be designed using current theoretical models along with experimentally determined properties. The application of bioresponsive hydrogels is wide ranging, and they have been developed into tissue engineering constructs, biosensors, and targeted drug delivery vehicles. Future developments will of necessity contain control loops similar to synthetic metabolic pathways. The use of these materials will continue to expand as they become coupled and integrated with new technologies.

CHAPTER 2: BIOACTIVE HYDROGELS DEMONSTRATE MEDIATED RELEASE OF A CHROMOPHORE BY CHYMOTRYPSIN

2.1. Introduction

A major challenge faced in drug delivery is administering a drug to a specific location at a controlled rate and amount. This is particularly challenging when the release rate and amount, must be controlled to a physiologically derived stimuli – so called bio-responsive drug delivery. To meet this challenge, biologically responsive hydrogels are being investigated as drug delivery vehicles [93, 119]. Since hydrogels can be tuned to be stimuli responsive and stimuli specific, they are attractive drug delivery systems because they can be tuned to deliver therapeutic molecules in a sustained or bolus type release [120], and do so in response to a biologically derived stimuli [121, 122]. Environmental [123], temperature [124] and pH-responsive hydrogels [75] have been designed by controlling solubility and ionic characteristics, and they have been successfully implemented in commercial applications [2, 125]. To increase the specificity of responsive hydrogels, bio-specific recognition agents have been combined with responsive hydrogels to create systems which sense and respond according to an engineered input[11, 38, 126-129]. Specifically, peptide sequences [130, 131] and enzymes have been used to provide biorecognition specificity[132]. Enzyme distributions may differ largely between healthy and diseased cells or biological systems [133, 134],

and this accordingly allows for the use of enzyme responsive hydrogels in disease targeting [2].

There are many possible designs of hydrogel drug delivery systems [11, 135, 136], and these are dictated by the specifics of the application. While not all hydrogel drug delivery systems can be improved by incorporating a bio-responsive component into the delivery scheme, cases do exist where vast improvements can be made. One such instance is the delivery of nerve growth factors (NGF). In work by Jhaveri et al. [137], poly(HEMA)-based hydrogels were loaded with NGFs by physical entrapment and subsequently released to promote neural growth around the hydrogel implant[137]. An improvement to this system would be the release of the growth factor triggered by cellular activity rather than the diffusivity rate of the entrapped NGF. This would enable the drug delivery rate to be mediated by biological (cellular) activity instead of by transport properties. Other studies have used Chondroitinase ABS, which degrades known neural growth inhibitors, to promote spinal cord recovery. Combining this enzyme with macroporous poly(HEMA)-based scaffolds used in spinal cord tissue engineering could improve the efficacy of such a system through release that was controlled by enzyme activity [138, 139]. Delivery systems may utilize different immobilization techniques, triggering mechanisms, and degradability. In previous work, we physically co-entrapped insulin and glucose oxidase (GOx) within poly(HEMA)-based hydrogel beads that included co-polymerized pH-responsive dimethylaminoethylmethacrylate (DMAEMA) monomer[3]. This molecularly engineered system clearly demonstrated programmed release of insulin mediated by the diffusion of glucose into the hydrogel. In

this system, the diffusing glucose was converted to gluconic acid via reaction with GOx. This caused an internal pH decrease that resulted in increased protonation of the tertiary amine, increased swelling of the hydrogel, and consequently, increased diffusivity of the peptide insulin out of the hydrogel; but not of GOx. The rate of insulin release could then be controlled by the bathing concentration of glucose.

To better understand the fundamental factors that control the release rate of a cleavable molecule from within a swellable hydrogel, a model system employing chymotrypsin as a surrogate for proteases and an enzyme cleavable chromogen, N-succinyl-Ala-Ala-Pro-Phe p-nitroanilide (Suc-AAPF-pNa) [140], was investigated. The hydrogel was a non-biodegradable, poly(HEMA)-based hydrogel that contained varying amounts of 2-aminoethyl methacrylate (AEMA) and was of variable cross-link density [141]. To study the release characteristics of this system, the release of the p-nitroanilide (pNa) chromophore was measured colorimetrically after the peptide sequence AAPF was cleaved by externally derived chymotrypsin. Cleavage causes the release of pNa and its subsequent colorimetric activation. To understand the influence of substrate loading by covalent conjugation, the AEMA content of the hydrogels was systematically varied. AEMA has a terminal primary amine group which is available for covalent conjugation with the chromogen. Varying the amount of primary amine groups within the hydrogel will therefore determine the amount of chromogen that can be covalently conjugated within the hydrogel. To understand the role of enzyme kinetics and/or mass transport effects as governing phenomena for the release rate, the cross-linked density of the hydrogel was likewise systematically varied. By systematically varying the cross-linker

concentration, the available void volume for transport is changed, and the effect this change has on the transport of the enzyme into the hydrogel can be studied. Following cleavage and release, the release rates were used to determine the Thiele moduli, which provided a novel approach to analyzing and optimizing the interactions of stimuli–causing enzymes within bio-responsive hydrogels. Through analysis of the determined Thiele moduli, the rate limiting process can be identified [142-144]. If mass transport limitations are governing the release, system parameters, specifically cross-linked density or the characteristic dimension, can be altered to avoid the limiting effects of mass transport which optimizes the release system.

2.2. Material and Methods

2.2.1 Hydrogel Disk Formulation and Characterization

The hydrogel components 2-hydroxyethylmethacrylate (HEMA), the divalent cross linker, tetraethyleneglycol diacrylate (TEGDA, technical grade), N-[tris(hydroxymethyl)methyl]-acrylamide (HMMA, 93%), poly(N-vinylpyrrolidone) (pNVP,MW=1,300,000), 2-aminoethyl methacrylate (AEMA), and the photoinitiator 2,2-dimethoxy-2-phenylacetophenone (DMPA, 99%) were purchased form Sigma Aldrich (Milwaukee, Wisconsin, USA). Prior to formulation, all of the liquid methacrylate and/or acrylate-containing reagents were passed over an inhibitor removal column (Sigma-Aldrich) to remove the polymerization inhibitors hydroquinone and/or monomethyl ether hydroquinone. Tris(hydroxymethyl)aminomethane (TRIS buffer, ACS reagent, 99.8+%,) was pH-adjusted with hydrochloric acid (ACS reagent, 37%) to obtain 0.1 M buffer of

pH = 7.4. Phosphate buffered saline (PBS) (1X, pH7.1) and 2-(N-morpholino) ethanesulfonic acid (MES Buffer, pH 4.7) were used. The peptide substrate, N-succinyl-Ala-Ala-Pro-Phe p-nitroanilide (CAS# 70967-97-4), and the enzyme, chymotrypsin (EC# 3.4.21.1), were purchased from Sigma–Aldrich (Milwaukee, Wisconsin, USA). Coupling reagents 1-ethyl-3-[3-dimethylaminopropyl] carbodiimide hydrochloride (EDC) and N-hydroxysulfosuccinimide sodium salt (Sulfo-NHS) were purchased from Thermo Scientific (Rockford, Illinois) and Sigma-Aldrich (Milwaukee, Wisconsin, USA), respectively. All solutions were prepared with deionized (MilliQ DI) water.

Bioactive p(HEMA)-based hydrogel pre-polymer cocktails were formulated by mixing the six constituents HEMA, TEGDA, HMMA, pNVP, DMPA, and AEMA with molar percentages outlined in Table 4 [145, 146]. HEMA was the primary monomer constituent and was chosen for its high hydration, non-biofouling, non-biodegradable characteristics. TEGDA was an effective cross linker that controlled the internal void volume. HMMA was used to increase hydrophilicity and hydration. pNVP was used to increase the viscosity of the monomer solution. DMPA was the photointiator for UV initiated polymerization of and acrylate and methacrylate groups. AEMA provided a reactive primary amine for covalent conjugation. Two sets of hydrogels were formulated; the first set varied AEMA mol% (Study A) and the second of varied TEDGA mol% (Study B). Gel formulations are summarized in Table 1.

Table 4: Hydrogel compositions for Studies A and B.

Monomer Component	Mol %	
	Study A	*Study B*
HEMA	91 - α	63 - β
TEGDA	3	β = 1, 5, 7, 9, 12
AEMA	α = 5, 10, 20, 30	30
HMMA	5	5
DMPA	1	1
p(NVP)	< 1	< 1

The pre-polymer mixtures were added to a 1:1 (v/v) solution of ethylene glycol/water to improve monomer solubility. The ethylene glycol/water mixed solvent was a total of 20 wt% of the final formulation. The solutions were mixed until all monomers had been dissolved and then sparged with nitrogen. An aliquot of 30 microliters of each hydrogel cocktail were evenly applied to silicone isolators, Figure 1, (664206, Grace Biolabs) of thickness 2.0 mm and diameter 4.5 mm. The mixtures were immediately UV irradiated (366 nm, 2.3 watts/cm^2, 5-7 min) in a UV cross-linker (CX-2000, UVP, Upland, CA, USA) under a flowing inert nitrogen atmosphere to effect polymerization of hydrogel discs. The resulting hydrogel discs were removed from the mold then simultaneously hydrated and solvent extracted. Hydration and solvent extraction was performed by sequential immersion in ethanol:PBS mixtures (75:25; 50:50 v/v) for a minimum of 1 h each and finally transferred to 100% PBS buffer. Sequential dilutions of ethanol were used to reduce the strain on the hydrogel disks which can lead to their cracking if the disks are placed directly into buffer. This procedure removed un-

reacted monomer that was not polymerized into the hydrogel backbone during polymerization, and it also replaced any residual ethylene glycol/water solvent with buffer.

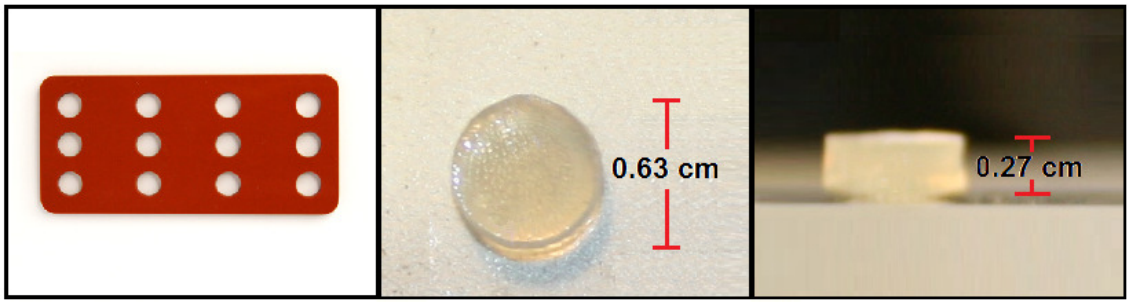

Figure 7: Silicone Isolator (Left), Hydrated 5% TEGDA/30% AEMA Hydrogel from Study B diameter (Center) and thickness (Right) dimensions.

The hydrated dimensions and void fractions of the hydrogels in Study B were experimentally determined. The physical dimensions of the hydrated gels were obtained by determining the hydrogel disk thickness and diameter using photographic dimensional analysis with ImageJ Software, Figure 7. Disk volume was calculated with diameter and thickness values by assuming cylindrical geometry. The masses of the hydrated and dehydrated gels were determined gravimetrically. The hydrogel discs were dehydrated (dried) in a Caliper-Zymark TurboVap 500 (Caliper Life Sciences, Hopkinton, MA, USA) and repeatedly weighed until a constant weight was achieved. The void fractions were calculated using Equation (42) where M_i is mass, HG is hydrated hydrogel, DG is dehydrated hydrogel, and ρ_i is density.

$$\varepsilon = \left(\frac{M_{HG} - M_{DG}}{\rho_{solution}}\right) / \left(\frac{M_{HG}}{\rho_{HG}}\right) \qquad (42)$$

Densities were calculated using mass and volume data obtained from photographic dimensional analysis and gravimetrical weights. This method for void

volume determination is similar to methods outlined by Karageorgiou [147]; however, only open voids, voids which water may access, are considered in this method. This is reasonable for this analysis as only voids filled by water will have enzymatically active chymotrypsin. The peptide conjugated chromogen, Suc-AAPF-pNa, was covalently linked to the fully hydrated and swollen hydrogel using EDC and Sulfo-NHS to couple the chromogen's carboxyl terminus to the primary amine group of AEMA which had been effectively cross-linked into the hydrogel and sits pendant to the backbone. To perform the covalent conjugation, Suc-AAPF-pNa was dissolved in MES buffer and centrifuged to remove any un-dissolved chromogen. The dissolved concentration was determined by UV-Vis spectroscopy. EDC was added to the dissolved chromogen solution creating a 1mM solution of EDC and allowed to incubate for 15 minutes to activate the carboxylic acid group on the chromogen. An aliquot of 0.3mL of the EDC/Chromogen solution was added to 0.9mL of a second solution containing the hydrogel disk and Sulfo-NHS in PBS. The final reaction solution contained 5mM Sulfo-NHS and was allowed to react for 2 hours under constant shaking. Following the conjugation reaction, the hydrogel discs were extracted into multiple changes of Tris/KCl/CaCl (100/100/50 mM at pH = 7.4) buffer to remove any un-conjugated, absorbed chromogen. The release of physically entrapped chromogen was monitored by assaying the solvent extract until no further chromogen release could be detected. This ensured that, once the hydrogel slab was placed in the chymotrypsin solution, any measured release of the chromogen was from the enzymatic cleavage of the peptide bond

of the covalently immobilized chromogen. This procedure was performed for both Study A and Study B and is illustrated in Figure 2.

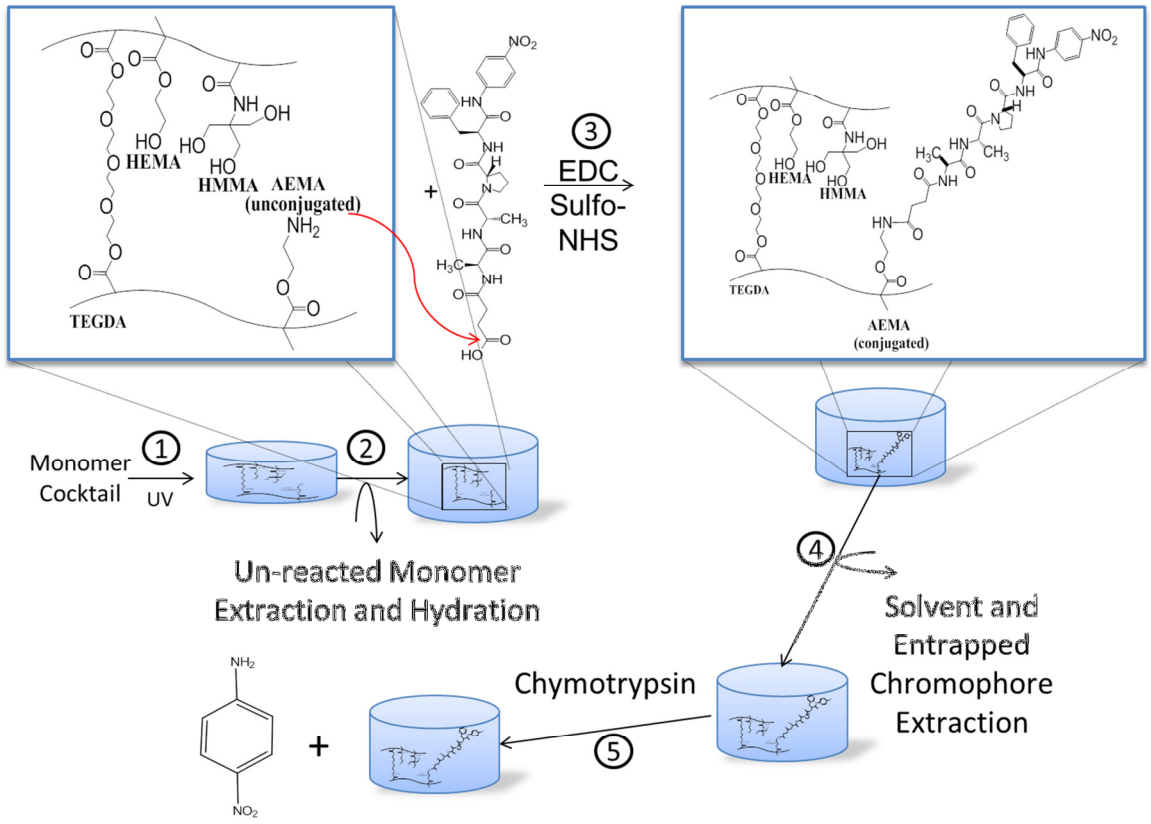

Figure 2: Schematic of hydrogel preparation and chromophore release process. (1) Cross-linking of hydrogel components to create disks. (2) Solvent extraction and hydration of hydrogel disks. (3) Covalently linkage of chromophore to hydrogel by EDC/Sulfo-NHS chemistry. (4) Removal of unreacted chromophore and reagents leaving only cross-linked chromophore. (5) Incubation of hydrogel disks in chymotrypsin solution releasing chromogen which is measured with UV-Vis spectroscopy.

2.2.2 Controlled Release of Chromophore from Hydrogel

Once all entrapped chromogen was removed, hydrogel discs were separately added to a continuously agitated 5 unit / mL solutions of chymotrypsin in Tris/KCl/CaCl (100/100/50 mM at pH = 7.4) buffer. The solution was periodically aliquoted and each

aliquot was analyzed by UV-Vis Spectroscopy using a Synergy Mx Monochromator-Based Multi-Mode Microplate Reader X (BioTek Instruments, Inc., Winooski, VT USA) to determine the concentration of the released chromophore. Samples were kept at constant volume by making up the removed volume from the sample with fresh buffer. Dilution of the solution was accounted for in concentration calculations.

2.2.3 Enzyme and Chromophore Characterization

In order to study the concentrations of the released chromophore a calibration curve (ranging from 0.0 - 0.40mM in 0.04mM increments) was created to confirm its extinction coefficient, and a spectrum scan from 230 to 900 nm wavelengths was performed to determine the peak absorbance. To measure the enzymatic activity of chymotrypsin with the targeted peptide sequence in the chromogen, initial enzymatic rate data were obtained for increasing concentrations (ranging from 0.010 - 0.100mM) of chromogen in Tris/KCl/CaCl buffer (100/100/50 mM at pH = 7.4 and T = 37^{o}C). A Lineweaver-Burke and Hill analysis was performed to determine the enzyme's catalytic constant, k_{cat}, the Michaelis constant, K_M, and the Hill exponent, n.

2.3. Results and Discussions

2.3.1 Enzyme and Chromophore Characterization

The determined extinction coefficient was 10,430 ± 90 $M^{-1}cm^{-1}$ at 380 nm, Figure 3 (Middle, imbedded). This value is similar to previously reported values of the extinction coefficient which was 9,900 $M^{-1}cm^{-1}$ at 410 nm [148]. Chymotrypsin is known to cleave preferentially at large aromatic peptides in the P1 position[149];

therefore Suc-AAPF-pNa was cleaved at Phe releasing the UV active p-Nitroanilide. The spectrum scan yielded only one peak which was associated with p-Nitroanilide. The concentrations of dissolved chromogen in the conjugating solution were determined to be 0.57mM and 0.20mM for studies A and B, respectively.

The experimentally determined values for chymotrypsin's kinetic parameters were, $k_{cat} = 9.39 \pm 0.63\ s^{-1}$, $K_M = 1.60x10^{-2} \pm 0.47x10^{-2}$ mM, and $n = 0.97 \pm 0.02$ (raw data not shown). These values differ from those found and reported by Wesolowska ($k_{cat} = 77s^{-1}$ and $K_M = 8.7\ x10^{-3}$ mM). The variations in k_{cat} and K_M may be attributed to different experimental temperatures (37^oC versus 22^oC), ion type (KCl versus NaCl), ion concentration, and/or pH(7.4 versus 8.4)[150].

2.3.2 Effect of Conjugating Amine Groups on Loading

Changes in chromogenic substrate loading were achieved by increasing the mol% of AEMA, which has an amine pendant group, within the hydrogel. Time-dependent cumulative release profiles, release rate, equilibrium concentrations, and Loading-Release Efficiency (E_{L-R}) all exhibited a positive correlation to increasing AEMA mol%, Figure 9. Figure 9A shows the kinetics of release of pNa as a function of the mol% of AEMA that was included in the hydrogel formulation. Both the initial rate of release and the amount released at t_∞, M_∞, show a clear dependence upon the mol% of AEMA, Figures 9A and 9B. Additionally, from Figure 9B, it is apparent that the increase in void fraction for hydrogels greater than 5% is negligible. This suggests there to be little effect on the D_{eff} for increasing AEMA mol%. Therefore for these hydrogels, the initial rate

increase can be attributed to greater substrate loading from more primary amine groups available for chromogen conjugation within the hydrogel.

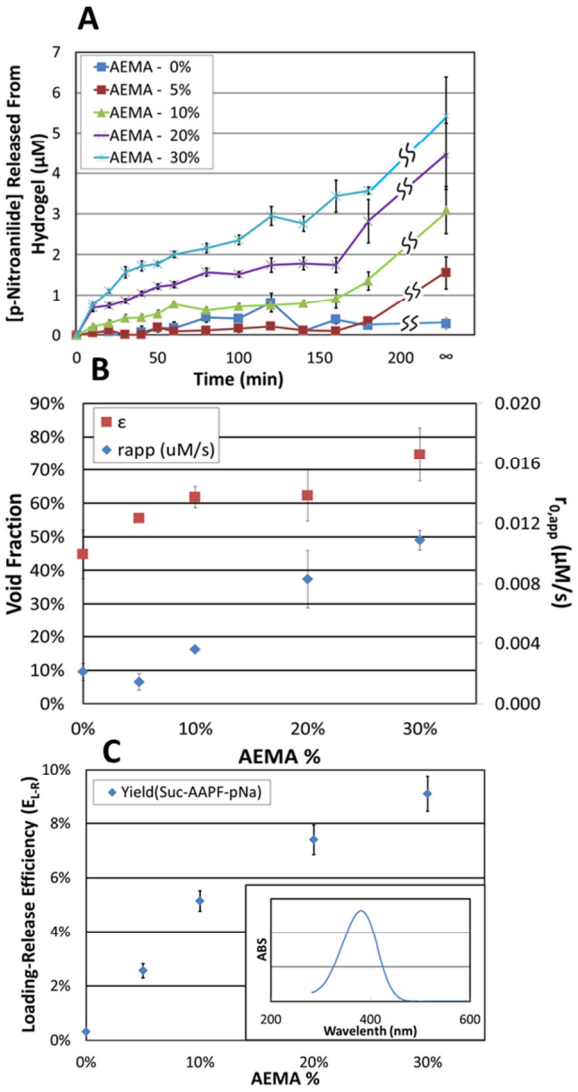

Figure 9: (A) A plot of the released concentration of chromophore after cleavage of its peptide sequence by chymotrypsin as a function AEMA mol%. (B) A plot of the void fraction (left y-axis) and release rate (right y-axis) as a function of AEMA mol%. (C) A plot of EL-R of the chromogen after cleavage of its conjugated peptide sequence by chymotrypsin as a function of AEMA mol%, and the spectrum scan of p-Nitroanilide after it has been cleaved from the peptide sequence.

The total amount of released chromophore from an enzymatically active substrate conjugated to a hydrogel matrix could be affected by the yield of the conjugation chemistry as well as by access of the enzyme to the covalently tethered substrate within the hydrogel. The peptide-to-hydrogel conjugation reaction will limit the amount of conjugated species through reaction equilibrium, and this in turn will influence the amount of subsequently released species. Additionally, only conjugated chromogen within voids to which the catalytically active enzyme has access could be potentially be released. Figure 9C shows the achieved Loading and Release Efficiency, $E_{L\text{-}R,}$ which was calculated using Equation (43).

$$E_{L-R} = \frac{M_{\infty}}{M_I} \times 100\% \qquad (43)$$

Where M_{∞} is the amount of released chromophore at equilibrium, and M_I is the amount of chromogen in the conjugating solution. This plot reflects the combined efficiency of peptide-to-hydrogel conjugation and release through enzymatic cleavage of a peptide bond as a function of increasing mol% of the conjugatable primary amine on AEMA.

It is not possible to distinguish from an examination of initial release rates or loading-release efficiencies if the conjugation reaction yield or enzymatic access to immobilized chromogen is limiting the amount of chromophore released from the hydrogels; however, the constant equilibrium values of released chromophore for varying mol% TEGDA, Table 4, provides some insight into the limiting factor. As cross-linked density is increased the hydrogel void volumes are reduced. If enzymatic access was affecting the amount of chromophore released from the hydrogels, it would be expected

that reducing the void volumes, effectively reducing voids within the hydrogel to which the enzyme has catalytic access, would reduce the final equilibrium value of released chromophore. This is not the case as there is no change in the final released amounts, M_∞, of the chromophore with increasing cross-link density. The fundamental factor controlling the loading is likely reaction equilibrium. As AEMA mol% is increased reaction equilibrium is forced further to the right resulting in high chromogen loading. Controlling reaction yield by a hydrogel monomer constituent, such as AEMA, may be a valuable approach if the species being conjugated is scarce in supply. This is often the case in biological applications as peptide motifs and other conjugated species are often associated with high cost and production time.

2.3.2 Effect of Cross-linked Density on Release

It may be desirable to control the release rate independent of substrate loading. To accomplish this, variations in enzyme access were controlled through the mol% of the cross-linker, TEDGA. Figure 10A shows a plot of the released concentration of chromophore following enzymatic cleavage of the peptide chromogen by chymotrypsin as a function TEGDA mol%. The cumulative release profiles of the chromophore showed a negative correlation with increasing TEGDA concentration. This is an expected result which is best analyzed qualitatively by considering forces at work within the system. Increasing TEGDA concentration, which controls the cross-link density, increases the onset of the retractive mechanical forces binding the polymer chain segments together. In opposition to the mechanical forces is the osmotic pressure difference between the hydrogel and bulk solution. As cross-linking increases, and consequently the mechanical

forces, the osmotic pressure is less able to drive water into the hydrogel resulting in a reduced degree of hydration. The reduction in hydration with increasing cross-linked density was measured experimentally and is reported in Table 5.

The reduction in hydration reduces the void volume of the hydrogel within which the catalytically active enzyme can diffuse and in so doing, the effective diffusivity of the enzyme through the hydrogel matrix is reduced. The reduction in effective diffusivity due to void fraction is commonly modeled using porous media model theory [119, 151]. The second parameter in the porous media model, Equation (44), which is affected by the cross-linked density is the tortuosity, τ, connecting the voids within the hydrogel.

$$D_{eff} = D_0 \frac{\varepsilon}{\tau} \tag{44}$$

$$\tau = \frac{L}{L_c} \tag{45}$$

As the cross-link density is increased the true molecular diffusion path length, L, increases relative to the length of the displacement path, L_c [152]. The increase in τ also contributes to the reduced effective diffusivities. Tortuosities were calculated using Equation (45) after effective diffusivities, D_{eff}, the diffusivity in buffer, D_0, and void fractions, ε, were determined. Figure 10B shows the effect of cross-linked density on ε and τ. By comparing the degree of change between ε and τ for increasing cross-linked density, it becomes apparent that increases in τ are the primary cause of a decreasing D_{eff} since τ increases two orders of magnitude over the range of TEGDA mol% while ε is reduced by only 50%.

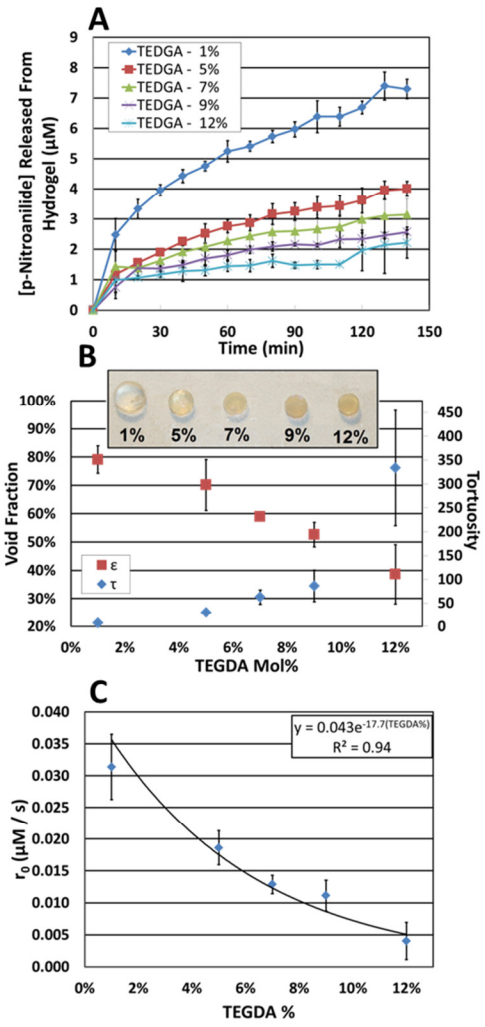

Figure 10: (A) A plot of the released concentration of chromophore after cleavage of its peptide sequence by chymotrypsin as a function TEGDA mol%. (B) A plot of the void fraction (left y-axis) and tortuosity (right y-axis) as a function of TEGDA mol%.. (C) A plot of the release rates of the chromophore after cleavage of its conjugated peptide sequence by chymotrypsin as a function of TEGDA mol%.

Figure 10C demonstrates the reduction in release rates that could be expected for increasing amounts of TEGDA. Following analysis which determined the system to be mass transport limited, the calculated release rates, shown in Figure 10C, were fit to an exponential decay. The observed changes in effective diffusivities were best fit by an

exponential decay, and thus, the release rates are expected to follow the same trend since mass transport is the limiting mechanism. To verify that cross-linked density was not affecting the loading of the chromogen the final released moles of chromophore, M_∞, were determined, Table 5. A constant amount of chromophore was released at equilibrium across varying cross-linked densities indicates the variations in cross-linked densities did not affect substrate loading.

Effective diffusivities of chymotrypsin through the hydrogel matrices were determined through a Thiele moduli analysis. Effectiveness factors and Thiele moduli were calculated using Equations (46) and (47) respectively [153], where η is the effectiveness factor, $r_{apparent}$ is the experimentally measured rate, and $r_{intrinsic}$ is the rate of reaction of the enzyme in a bulk solution of substrate. Effectiveness factors were determined from experimentally determined initial rates $r_{0,apparent,}$ and theoretical intrinsic rates, $r_{0,intrinsic}$, determined from Equation (48).

$$\eta \equiv \frac{r_{apparent}}{r_{intrinsic}} \tag{46}$$

$$\eta = \left(\frac{1}{\varphi}\right)\left(\frac{1}{\tanh(3\varphi)} - \frac{1}{3\varphi}\right) \tag{47}$$

For the intrinsic rate calculation, the previously determined V_{max} and K_M were used in Equation (48), and the initial concentrations of the covalently attached substrate, [M*], were approximated by Equation (49). There was an observed increase in the values of [M*] for increasing cross-linked density; however, this can be attributed to the decreasing hydrogel volume, that is, less swelling of the hydrogel since, M_∞, was constant across cross-linked densities.

$$r_{0,intrinsic} = \frac{V_{max}[M^*]}{K_M + [M^*]} \quad (48)$$

$$[M^*] = \frac{V_{solution}[M_\infty]}{V_{gel}\varepsilon} \quad (49)$$

The Thiele moduli shown in Table 5 were in all cases >> 1 which is characteristic of extremely mass transport limited system [154]. Since the release requires a large molecule, chymotrypsin (25 kDa), to diffuse into the hydrogel, the mass transport limiting characteristic of this system is expected. The effective diffusivity constants, D_{eff}, for varying cross-link density were then calculated by Equation (50)

$$\varphi = \frac{R}{\alpha}\left[\frac{V_{max}}{K_M D_{eff}}\right]^{1/2} \quad (50)$$

Where R is the characteristic length, α is 2 (α = 1, 2, or 3 for slabs, cylinders, or spheres, respectively) [144], φ is the Thiele modulus, and K_M and V_{max} are the enzyme kinetic constants. The values of these calculations are summarized in Table 5.

Table 5: Calculated parameters for varying cross-linked densities determined from the analysis of experimentally measured rate data.

TEGDA	Degree of Hydration	M_∞	$r_{0,apparent}$	$r_{0,intrinsic}$	η x10^3	φ	D_{eff}
(mol %)	*(%)*	*(μmols)*	*(μM s^{-1})*	*(μM s^{-1})*	*(%)*	*(-)*	*(cm^2 s^{-1})*
1%	82.0 ± 0.1	10.8 ± 1.3	0.0314 ± 0.0051	29.9 ± 0.2	1.05 ± 0.17	965 ± 147	6.9x10^{-8} ± 2.2x10^{-8}
5%	67.5 ± 0.4	10.9 ± 1.3	0.0186 ± 0.0027	31.1 ± 0.0	0.60 ± 0.09	1690 ± 227	1.4x10^{-8} ± 0.4x10^{-8}
7%	61.6 ± 0.4	9.5 ± 1.1	0.0129 ± 0.0014	31.3 ± 0.0	0.41 ± 0.05	2450 ± 291	0.6x10^{-8} ± 0.1x10^{-8}
9%	55.8 ± 1.7	10.2 ± 0.2	0.0111 ± 0.0024	31.3 ± 0.0	0.35 ± 0.08	2889 ± 586	0.4x10^{-8} ± 0.2x10^{-8}
12%	50.7 ± 0.5	10.2 ± 1.9	0.0054 ± 0.0017	31.4 ± 0.0	0.17 ± 0.05	5979 ± 1908	0.1x10^{-8} ± 0.1x10^{-8}

D_0 of chymotrypsin was calculated using an empirical fit to the effective diffusivities *vs.* Degree of Hydration and extrapolating to 100% hydration, representing pure buffer solution. Degree of Hydration was calculated using Equation (51) [145].

$$\text{Degree of Hydration (\%)} = \frac{M_{HG} - M_{DG}}{M_{HG}} \times 100\% \qquad (51)$$

The D_0 value determined in this way was found to be $6.9 \pm 0.5 \times 10^{-7}$ cm^2 s^{-1}. This value is only slightly larger when compared to $5.3 \pm 0.2 \times 10^{-7}$ cm^2 s^{-1} determined for a simple phosphated adduct of the 25kDa chymotrypsin [155, 156]. The small increase may be due to the partitioning of chymotrypsin into the hydrogel. The partition coefficient for chymotrypsin into the poly(HEMA)-based hydrogel was not determined for this work; however, Equation (44) can be modified to account for this effect by including a partition coefficient, K_p, Equation (52).

$$D_{eff} = K_P D_0' \frac{\varepsilon}{\tau} \qquad (52)$$

Without determining the partitioning coefficient, the calculated D_0 value is a lumped parameter equal to the multiple of D_0' and K_p, and it includes any partitioning effects. The contribution of this effect is believed to be small because the D_0 in this work is similar to that of others. The diffusion rate of chymotrypsin in an uncrosslinked polymer was calculated using an empirical fit to the effective diffusivities *vs.* TEGDA mol% and was determined to be $9.5 \pm 0.3 \times 10^{-5}$ cm^2 s^{-1}. These values are akin to the diffusivity of chymotrypsin within crowded media [156].

2.3.3 Using Thiele Moduli to Optimize Drug Delivery Systems

In the design of biologically responsive hydrogel drug delivery systems within which proteases are used to cleave and hence initiate and provoke a release response, Equation (50) may be used to optimize critical parameters for such systems. The optimal system will be one in which the release rate is kinetically limited, that is, when $\varphi << 1$ [154]. To illustrate analysis of such a system, the case where $r_{apparent}$ is 99% of $r_{intrinsic}$ will be considered (i.e. η=0.99, φ=0.13). Breaking the equation into biological intrinsic properties, V_{max} and K_M, and design parameters, R, α, and D_{eff}, allows a maximum value of R to be calculated where mass transport is not limiting, $(R\ \alpha^{-1})_{max}$. R is the characteristic dimension of the system; for slabs it is the length of the dimension parallel to the direction of transport and for cylinders and spheres it is the radii. α is a constant resulting from the derivation of Equation (50) and has a value of 1, 2, or 3 for slab, cylindrical, or spherical geometries, respectively. Figure 5 demonstrates this relationship for varying effective diffusivities of the protease enzyme.

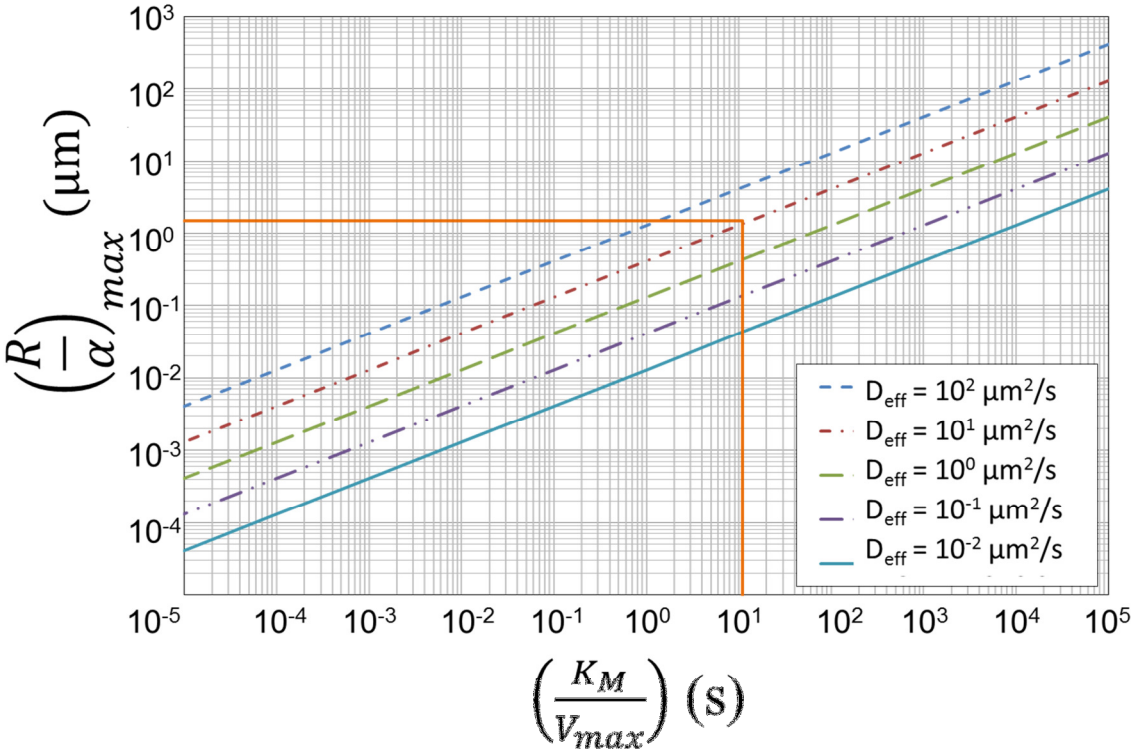

Figure 11: A plot of the maximum characteristic dimension of a hydrogel which will not have mass transport limitations as a function of effective diffusivity and K_M V_{max}^{-1}.

To illustrate how Figure 10 may be used to optimize a bio-responsive hydrogel which uses enzymatic cleavage for release, consider the case of the 5 mol% TEGDA cross-linked hydrogel disks in this study. For this composition the ratio of $K_M V_{max}^{-1}$ is calculated to be 10.9 seconds. The effective diffusivity for these disks was 1.4×10^{-8} cm^2/s. From Figure 10, this corresponds to a $(R\ \alpha^{-1})_{max}$ value of 1.5 μm. For the cylindrical geometry of our discs $\alpha = 2$, so the optimized cylinder would have a radii of 0.75 μm. A similar analysis could be performed on planar ($\alpha = 1$) or spherical ($\alpha = 3$) geometries. Bio-responsive hydrogel spheres and thin films used in biological applications could benefit from such an analysis since altering the characteristic dimension could move the system from mass transport limited to a kinetically limited

regime. This would maximize the release rate from the hydrogel which is one of the most significant weaknesses of these systems [76].

2.4. Remarks and Conclusions

The release of the chromophore, a surrogate for a drug, in this study occurred by the diffusion of the protease enzyme into a poly(HEMA)-based hydrogel, and then by the subsequent enzymatic cleavage of a targeted peptide sequence caused the release of an elutable chromophore from the hydrogel network. The rate-limiting step in this process will typically be mass transport due to the low effective diffusivities of large proteases into the hydrogel; however, the hydrogel size, shape, and cross-linked density may serve as design criteria with which to balance or remove the transport limitations in order to achieve programmed release from such systems. While this work used a chromophore and the enzyme chymotrypsin, similar systems could be designed using therapeutic drugs and other specific proteases in lieu of these molecules.

The amount of an enzymatically active substrate loaded into a hydrogel matrix can be controlled by varying the amount of conjugating monomer that is polymerized into the hydrogel backbone. The amount of the substrate loaded and released would then depend upon the conjugation chemistry as well as enzymatic access to the covalently bound substrate; however, the loading in this study was found to depend primarily on the equilibrium of the conjugation chemistry. For systems which have lower hydrogel void fractions (<40%) or are using large proteins (>25kDa), enzyme access may need to be considered in yield calculations. The release rate from the hydrogel after cleavage was

affected by both the amount of hydrophilic, conjugating monomer and cross-linked density. To control the release rate cross-linked density can be changed without affecting the substrate loading. In targeted drug-delivery, controlling the amount of drug delivered and rate at which it is delivered independently can serve as a valuable design methodology. This study investigated a methodology of engineering a bio-responsive hydrogel which could achieve this goal.

CHAPTER 3: FUTURE WORK

The goal of future work in enzymatically actuated bioresponsive hydrogels will be continued investigation of methods and theories which will allow for better control over sensing, transduction, and response in these materials. To this end, pre-polymerization loading methodologies will be investigated *in vitro*, *in silico* diffusion-reaction multiphysics modeling will be performed to match experimental data, and enzyme actuated degradation of the polymer will be engineered as a material capability.

Pre-polymerization loading will involve the synthesis of acryolyl-peptide conjugates; its subsequent separation, purification, and analysis; and finally, its inclusion into the monomer cocktail prior to UV polymerization of the matrix. Pre-polymerization loading may allow for higher loading efficiencies and/or further investigation into the conjugates' *in vitro* properties (i.e. enzyme kinetic parameters for the solution phase conjugate). Therefore, pre-loaded hydrogels will be synthesized and the results will be compared to the previously discussed study in Chapter 2 to interrogate pros and cons of both methods.

In silico modeling of enzymatically actuated hydrogels will be investigated. These models will serve as confirmation to the theories of kinetic, thermodynamic, and transport phenomena. Additionally, they will serve as optimization and experimental guidance tools for other systems wherein system parameters (ie. K_M, k_{cat} $[E]_T$, $[M^*]$, D_{eff}, etc.) could be altered. COMSOL Multiphysics will be used as the primary modeling

software. Transport models discussed in Chapter 1 will be used in conjugation with the FEM models and experimental data.

Creating a hydrogel which is able to degrade in response to enzyme activity will be a final goal of future work. In order to confer erosion capabilities to the polymer backbone the labile cross-linker, TEGDA, will be substituted by a diacrylate-peptide that is enzymatically active. The work outline in Chapter 2 demonstrated enzyme diffusion control by varying cross-linking concentration. As the concentration of cross-linker is increased diffusion of proteases diffusivity constants drop exponentially. This will subsequently reduce the amount of enzyme available to cleaving the backbone-integrated peptide and reduce the rate of erosion; however, as concentration of erodible cross-linker increases the number of cleavable sites will increase, thus increasing the rate of erosion. These competing phenomena generate a high order of complexity in understanding how to control erosion rates. Investigation of this system will proceed by experimental degradation by enzymatic erosion and subsequently the erosion rates will be analyzed in view of surface, bulk, or moving front erosion theories.

This work will contribute to the core understanding of increasingly complex bioresponsive hydrogel systems. It will serve as platform theories and methods for applications in drug delivery, sensors, and tissue engineering. The continued integration of bioresponsive hydrogels guarantees the demand and need for sustained research and development in this field, and it promises to deliver technologies which will better serve civilian, military, and medical industries.

REFERENCES

1. Gawel, K., et al., *Responsive Hydrogels for Label-Free Signal Transduction within Biosensors.* Sensors, 2010. **10**(5): p. 4381-4409.
2. Ulijn, R.V., et al., *Bioresponsive hydrogels.* Materials Today, 2007. **10**(4): p. 40-48.
3. Guiseppi-Elie, A., S. Brahim, and D. Narinesingh, *A chemically synthesized artificial pancreas: Release of insulin from glucose–responsive hydrogels.* Advanced Materials, 2002. **14**(10): p. 743-46.
4. Wilson, A.N., R. Salas, and A. Guiseppi-Elie, *Bioactive hydrogels demonstrate mediated release of a chromophore by chymotrypsin.* Journal of Controlled Release, 2012. **(in press)**.
5. Fischel-Ghodsian, F., et al., *Enzymatically controlled drug delivery.* Proceedings of the National Academy of Sciences, 1988. **85**(7): p. 2403-2406.
6. Yamaguchi, N., et al., *Growth Factor Mediated Assembly of Cell Receptor-Responsive Hydrogels.* Journal of the American Chemical Society, 2007. **129**(11): p. 3040-3041.
7. Lee, K.Y. and D.J. Mooney, *Hydrogels for Tissue Engineering.* Chemical Reviews, 2001. **101**(7): p. 1869-1880.
8. Yu, H. and D.W. Grainger, *Thermo-sensitive swelling behavior in crosslinked N-isopropylacrylamide networks: Cationic, anionic, and ampholytic hydrogels.* Journal of Applied Polymer Science, 1993. **49**(9): p. 1553-1563.
9. Suzuki, Y., et al., *Change in phase transition behavior of an NIPA gel induced by solvent composition: hydrophobic effect.* Polymer Gels and Networks, 1996. **4**(2): p. 129-142.
10. Miyata, T., N. Asami, and T. Uragami, *A reversibly antigen-responsive hydrogel.* Nature, 1999. **399**(6738): p. 766-769.
11. Thornton, P.D., R.J. Mart, and R.V. Ulijn, *Enzyme-Responsive Polymer Hydrogel Particles for Controlled Release.* Advanced Materials, 2007. **19**(9): p. 1252-1256.
12. Nicodemus, G.D. and S.J. Bryant, *Cell Encapsulation in Biodegradable Hydrogels for Tissue Engineering Applications.* Tissue Engineering Part B: Reviews, 2008. **14**(2): p. 149-165.
13. Wang, D.-A., et al., *Bioresponsive Phosphoester Hydrogels for Bone Tissue Engineering.* Tissue Engineering, 2005. **11**(1-2): p. 201-213.
14. Yang, H., et al., *Engineering Target-Responsive Hydrogels Based on Aptamer−Target Interactions.* Journal of the American Chemical Society, 2008. **130**(20): p. 6320-6321.
15. Pillai, O. and R. Panchagnula, *Polymers in drug delivery.* Current Opinion in Chemical Biology, 2001. **5**(4): p. 447-451.
16. Huang, X. and T.L. Lowe, *Biodegradable Thermoresponsive Hydrogels for Aqueous Encapsulation and Controlled Release of Hydrophilic Model Drugs.* Biomacromolecules, 2005. **6**(4): p. 2131-2139.
17. Hendrickson, G.R. and L. Andrew Lyon, *Bioresponsive hydrogels for sensing applications.* Soft Matter, 2009. **5**(1): p. 29-35.

18. Guiseppi-Elie, A., *Electroconductive hydrogels: Synthesis, characterization and biomedical applications.* Biomaterials, 2010. **31**(10): p. 2701-2716.
19. Bird, S.P. and L.A. Baker, *Biologically modified hydrogels for chemical and biochemical analysis.* Analyst, 2011.
20. Pinto, J.F., *Site-specific drug delivery systems within the gastro-intestinal tract: From the mouth to the colon.* International Journal of Pharmaceutics, 2010. **395**(1–2): p. 44-52.
21. Ganji, F. and E. Vasheghani-Farahani, *Hydrogels in controlled drug delivery systems.* Iran Polym J, 2009. **18**: p. 63-88.
22. Wolfe, D., M. Mata, and D.J. Fink, *Targeted drug delivery to the peripheral nervous system using gene therapy.* Neuroscience Letters, (0).
23. Meng, F., Z. Zhong, and J. Feijen, *Stimuli-responsive polymersomes for programmed drug delivery.* Biomacromolecules, 2009. **10**(2): p. 197-209.
24. Li, J., et al., *Label-free colorimetric detection of trace cholesterol based on molecularly imprinted photonic hydrogels.* Journal of Materials Chemistry, 2011. **21**(48): p. 19267-19274.
25. Kapellos, G.E., T.S. Alexiou, and A.C. Payatakes, *A multiscale theoretical model for fluid flow in cellular biological media.* International Journal of Engineering Science, 2012. **51**(0): p. 241-271.
26. Lin, C.C. and A.T. Metters, *Hydrogels in controlled release formulations: network design and mathematical modeling.* Advanced Drug Delivery Reviews, 2006. **58**(12): p. 1379-1408.
27. Li, H., J. Chen, and K. Lam, *Multiphysical modeling and meshless simulation of electric-sensitive hydrogels.* Journal of Polymer Science Part B: Polymer Physics, 2004. **42**(8): p. 1514-1531.
28. Casault, S. and G.W. Slater, *Systematic characterization of drug release profiles from finite-sized hydrogels.* Physica A: Statistical Mechanics and its Applications, 2008. **387**(22): p. 5387-5402.
29. Pandis, C., et al., *Water sorption characteristics of poly(2-hydroxyethyl acrylate)/silica nanocomposite hydrogels.* Journal of Polymer Science Part B: Polymer Physics, 2011. **49**(9): p. 657-668.
30. Jin, R., et al., *Enzyme-mediated fast in situ formation of hydrogels from dextran-tyramine conjugates.* Biomaterials, 2007. **28**(18): p. 2791-2800.
31. Lévesque, S.G. and M.S. Shoichet, *Synthesis of Enzyme-Degradable, Peptide-Cross-Linked Dextran Hydrogels.* Bioconjugate Chemistry, 2007. **18**(3): p. 874-885.
32. Miyata, T., N. Asami, and T. Uragami, *Preparation of an Antigen-Sensitive Hydrogel Using Antigen−Antibody Bindings.* Macromolecules, 1999. **32**(6): p. 2082-2084.
33. Murakami, Y. and M. Maeda, *DNA-Responsive Hydrogels That Can Shrink or Swell.* Biomacromolecules, 2005. **6**(6): p. 2927-2929.
34. Miyata, *Preparation of reversibly glucose-responsive hydrogels by covalent immobilization of lectin in polymer networks having pendant glucose.* Journal of Biomaterials Science, Polymer Edition, 2004. **15**: p. 1085-1098.

35. Lutolf, M.P., et al., *Synthetic matrix metalloproteinase-sensitive hydrogels for the conduction of tissue regeneration: Engineering cell-invasion characteristics.* Proceedings of the National Academy of Sciences, 2003. **100**(9): p. 5413-5418.
36. Jang, E., et al., *Fabrication of poly(ethylene glycol)-based hydrogels entrapping enzyme-immobilized silica nanoparticles.* Polymers for Advanced Technologies, 2010. **21**(7): p. 476-482.
37. Lee, S.B. and K.-J. Kim, *Effect of water activity on enzyme hydration and enzyme reaction rate in organic solvents.* Journal of Fermentation and Bioengineering, 1995. **79**(5): p. 473-478.
38. Podual, K., F.J. Doyle, and N.A. Peppas, *Preparation and dynamic response of cationic copolymer hydrogels containing glucose oxidase.* Polymer, 2000. **41**(11): p. 3975-3983.
39. Chauhan, G.S., et al., *Immobilization of lipase on hydrogels: Structural aspects of polymeric matrices as determinants of enzyme activity in different physical environments.* Journal of Applied Polymer Science, 2004. **92**(5): p. 3135-3143.
40. am Ende, M.T. and N.A. Peppas, *Transport of ionizable drugs and proteins in crosslinked poly(acrylic acid) and poly(acrylic acid-co-2-hydroxyethyl methacrylate) hydrogels. II. Diffusion and release studies.* Journal of Controlled Release, 1997. **48**(1): p. 47-56.
41. Ganji, F. and E. Vasheghani-Farahani, *THEORETICAL DESCRIPTION OF HYDROGEL SWELLING: A REVIEW.* Iranian Polymer Journal, 1998. **19**(5): p. 1026-1265.
42. Yan, Q. and A.S. Hoffman, *Synthesis of macroporous hydrogels with rapid swelling and deswelling properties for delivery of macromolecules.* Polymer, 1995. **36**(4): p. 887-889.
43. Brahim, S. and A. Guiseppi-Elie, *Electroconductive Hydrogels: Electrical and Electrochemical Properties of Polypyrrole-Poly(HEMA) Composites.* Electroanalysis, 2005. **17**(7): p. 556-570.
44. Ramanathan, S. and L.H. Block, *The use of chitosan gels as matrices for electrically-modulated drug delivery.* Journal of Controlled Release, 2001. **70**(1-2): p. 109-123.
45. Crank, J., *The mathematics of diffusion*. Vol. 1. 1979: Clarendon press Oxford.
46. Amsden, B., *Solute Diffusion within Hydrogels. Mechanisms and Models.* Macromolecules, 1998. **31**(23): p. 8382-8395.
47. Cohen, M.H. and D. Turnbull, *Molecular transport in liquids and glasses.* The Journal of Chemical Physics, 1959. **31**: p. 1164.
48. Truskey, G.A., F. Yuan, and D.F. Katz, *Transport phenomena in biological systems*2004: Pearson/Prentice Hall.
49. Yasuda, H., et al., *Permeability of solutes through hydrated polymer membranes. Part III. Theoretical background for the selectivity of dialysis membranes.* Die Makromolekulare Chemie, 1969. **126**(1): p. 177-186.
50. Lustig, S.R. and N.A. Peppas, *Solute diffusion in swollen membranes. IX. Scaling laws for solute diffusion in gels.* Journal of Applied Polymer Science, 1988. **36**(4): p. 735-747.

51. Peppas, N.A. and E.W. Merrill, *Poly(vinyl alcohol) hydrogels: Reinforcement of radiation-crosslinked networks by crystallization.* Journal of Polymer Science: Polymer Chemistry Edition, 1976. **14**(2): p. 441-457.
52. Peppas, N., et al., *Hydrogels in pharmaceutical formulations.* European Journal of Pharmaceutics and Biopharmaceutics, 2000. **50**(1): p. 27-46.
53. Peppas, N.A. and N.K. Mongia, *Ultrapure poly (vinyl alcohol) hydrogels with mucoadhesive drug delivery characteristics.* European Journal of Pharmaceutics and Biopharmaceutics, 1997. **43**(1): p. 51-58.
54. Stauffer, S.R. and N.A. Peppast, *Poly (vinyl alcohol) hydrogels prepared by freezing-thawing cyclic processing.* Polymer, 1992. **33**(18): p. 3932-3936.
55. Peppas, N.A., *Hydrogels in medicine and pharmacy : vol. 2 polymers*1987, Boca Raton, Fla.: CRC Press.
56. Ahuja, N., O.P. Katare, and B. Singh, *Studies on dissolution enhancement and mathematical modeling of drug release of a poorly water-soluble drug using water-soluble carriers.* European Journal of Pharmaceutics and Biopharmaceutics, 2007. **65**(1): p. 26-38.
57. Ritger, P.L. and N.A. Peppas, *A simple equation for description of solute release I. Fickian and non-fickian release from non-swellable devices in the form of slabs, spheres, cylinders or discs.* Journal of Controlled Release, 1987. **5**(1): p. 23-36.
58. Peppas, N.A. and J.J. Sahlin, *A simple equation for the description of solute release. III. Coupling of diffusion and relaxation.* International Journal of Pharmaceutics, 1989. **57**(2): p. 169-172.
59. Siepmann, J. and F. Siepmann, *Modeling of diffusion controlled drug delivery.* Journal of Controlled Release, 2011.
60. Omidian, H., J.G. Rocca, and K. Park, *Advances in superporous hydrogels.* Journal of Controlled Release, 2005. **102**(1): p. 3-12.
61. Murdan, S., *Electro-responsive drug delivery from hydrogels.* Journal of Controlled Release, 2003. **92**(1-2): p. 1-17.
62. Wallmersperger, *Coupled chemo-electro-mechanical finite element simulation of hydrogels: II. Electrical Simulation.* Smart Materials and Structures, 2008. **17**(4).
63. Siegel, R.A. and B.A. Firestone, *pH-dependent equilibrium swelling properties of hydrophobic polyelectrolyte copolymer gels.* Macromolecules, 1988. **21**(11): p. 3254-3259.
64. Prausnitz, J.M., R.N. Lichtenthaler, and E.G. Azevedo, *Molecular thermodynamics of fluid-phase equilibria*1999: Prentice-Hall PTR.
65. Fried, J.R., *Conformation, solutions and molecular weight.* , in *Polymer science and technology*, J.R. Fried, Editor 2003, Prentice Hall PTR: Englewood Cliffs, NJ, . p. 582.
66. Krevelen, W. and K.t. Nijenhuis, *Properties of Polymers: Their Correlation with Chemical Structure; Their Numerical Estimation and Prediction from Additive Group Contributions*. 4th ed2009, Amsterdam: Elsevier Science Publishers BU. 1004.
67. Ganji, F., S. Vasheghani-Farahani, and E. Vasheghani-Farahani, *Theoretical description of hydrogel swelling: a review.* Iran Polym J, 2010. **19**(5): p. 375-398.

68. Davis, T.P. and M.B. Huglin, *Effect of composition on properties of copolymeric N-vinyl-2-pyrrolidonemethyl methacrylate hydrogels and organogels.* Polymer, 1990. **31**(3): p. 513-519.
69. Wang, J., W. Wu, and Z. Lin, *Kinetics and thermodynamics of the water sorption of 2-hydroxyethyl methacrylate/styrene copolymer hydrogels.* Journal of Applied Polymer Science, 2008. **109**(5): p. 3018-3023.
70. Marchetti, M., S. Prager, and E.L. Cussler, *Thermodynamic predictions of volume changes in temperature-sensitive gels. 1. Theory.* Macromolecules, 1990. **23**(6): p. 1760-1765.
71. Flory, P.J., R.A. Orwoll, and A. Vrij, *Statistical Thermodynamics of Chain Molecule Liquids. II. Liquid Mixtures of Normal Paraffin Hydrocarbons.* Journal of the American Chemical Society, 1964. **86**(17): p. 3515-3520.
72. Peppas, N.A. and E.W. Merrill, *Crosslinked poly (vinyl alcohol) hydrogels as swollen elastic networks.* Journal of Applied Polymer Science, 1977. **21**(7): p. 1763-1770.
73. Safranski, D.L., et al., *Effect of poly (ethylene glycol) diacrylate concentration on network properties and in vivo response of poly (β-amino ester) networks.* Journal of Biomedical Materials Research Part A, 2011. **96**(2): p. 320-329.
74. Pishko, M.V., A.C. Michael, and A. Heller, *Amperometric glucose microelectrodes prepared through immobilization of glucose oxidase in redox hydrogels.* Analytical Chemistry, 1991. **63**(20): p. 2268-2272.
75. Brahim, S., D. Narinesingh, and A. Guiseppi-Elie, *Release characteristics of novel pH-sensitive p(HEMA-DMAEMA) hydrogels containing 3-(trimethoxy-silyl) propyl methacrylate.* Biomacromolecules, 2003. **4**(5): p. 1224-1231.
76. Qiu, Y. and K. Park, *Environment-sensitive hydrogels for drug delivery.* Advanced Drug Delivery Reviews, 2001. **53**(3): p. 321-339.
77. Fogler, H.S., *Elements of chemical reaction engineering*1999: Prentice Hall PTR.
78. Toledano, S., et al., *Enzyme-Triggered Self-Assembly of Peptide Hydrogels via Reversed Hydrolysis.* Journal of the American Chemical Society, 2006. **128**(4): p. 1070-1071.
79. Horkay, F., I. Tasaki, and P.J. Basser, *Osmotic Swelling of Polyacrylate Hydrogels in Physiological Salt Solutions.* Biomacromolecules, 2000. **1**(1): p. 84-90.
80. Chang, C., et al., *Superabsorbent hydrogels based on cellulose for smart swelling and controllable delivery.* European Polymer Journal, 2010. **46**(1): p. 92-100.
81. Kelmanovich, S.G., R. Parke-Houben, and C.W. Frank, *Competitive swelling forces and interpolymer complexation in pH-and temperature-sensitive interpenetrating network hydrogels.* Soft Matter, 2012.
82. Li, H., et al., *Modeling and Simulation of the Swelling Behavior of pH-Stimulus-Responsive Hydrogels.* Biomacromolecules, 2004. **6**(1): p. 109-120.
83. Wallmersperger, T., et al., *Coupled multi-field formulation in space and time for the simulation of intelligent hydrogels.* Journal of Intelligent Material Systems and Structures, 2009. **20**(12): p. 1483-1492.

84. Kang, B., et al., *Dynamical modeling and experimental evidence on the swelling/deswelling behaviors of pH sensitive hydrogels.* Materials Letters, 2008. **62**(19): p. 3444-3446.
85. Wallmersperger, T., et al., *Modeling and simulation of pH-sensitive hydrogels.* Colloid & Polymer Science, 2011. **289**(5): p. 535-544.
86. Riedinger, A., et al., *"Nanohybrids" Based on pH-Responsive Hydrogels and Inorganic Nanoparticles for Drug Delivery and Sensor Applications.* Nano Letters, 2011. **11**(8): p. 3136-3141.
87. Chen, Z., et al., *pH-Sensitive Water-Soluble Nanospheric Imprinted Hydrogels Prepared as Horseradish Peroxidase Mimetic Enzymes.* Advanced Materials, 2010. **22**(13): p. 1488-1492.
88. Sabir, M., X. Xu, and L. Li, *A review on biodegradable polymeric materials for bone tissue engineering applications.* Journal of Materials Science, 2009. **44**(21): p. 5713-5724.
89. Martina, M. and D.W. Hutmacher, *Biodegradable polymers applied in tissue engineering research: a review.* Polymer International, 2007. **56**(2): p. 145-157.
90. Göpferich, A. and J. Tessmar, *Polyanhydride degradation and erosion.* Advanced Drug Delivery Reviews, 2002. **54**(7): p. 911-931.
91. Middleton, J.C. and A.J. Tipton, *Synthetic biodegradable polymers as orthopedic devices.* Biomaterials, 2000. **21**(23): p. 2335-2346.
92. Atzet, S., et al., *Degradable Poly(2-hydroxyethyl methacrylate)-co-polycaprolactone Hydrogels for Tissue Engineering Scaffolds.* Biomacromolecules, 2008. **9**(12): p. 3370-3377.
93. Aimetti, A.A., A.J. Machen, and K.S. Anseth, *Poly(ethylene glycol) hydrogels formed by thiol-ene photopolymerization for enzyme-responsive protein delivery.* Biomaterials, 2009. **30**(30): p. 6048-6054.
94. Wilson, A.N., R. Salas, and A. Guiseppi-Elie, *Bioactive hydrogels demonstrate mediated release of a chromophore by chymotrypsin.* J Control Release, 2012. **160**(1): p. 41-7.
95. Brandl, F.P., et al., *Enzymatically degradable poly(ethylene glycol) based hydrogels for adipose tissue engineering.* Biomaterials, 2010. **31**(14): p. 3957-3966.
96. Yong, V.W., *Metalloproteinases in biology and pathology of the nervous system.* Nature Reviews Neuroscience, 2001. **2**(7): p. 502.
97. Lynn, D.M., M.M. Amiji, and R. Langer, *pH-Responsive Polymer Microspheres: Rapid Release of Encapsulated Material within the Range of Intracellular pH.* Angewandte Chemie, 2001. **113**(9): p. 1757-1760.
98. Saito, G., J.A. Swanson, and K.-D. Lee, *Drug delivery strategy utilizing conjugation via reversible disulfide linkages: role and site of cellular reducing activities.* Advanced Drug Delivery Reviews, 2003. **55**(2): p. 199-215.
99. Wei, H., et al., *Self-assembled, thermosensitive micelles of a star block copolymer based on PMMA and PNIPAAm for controlled drug delivery.* Biomaterials, 2007. **28**(1): p. 99-107.

100. Lensen, D., et al., *Biodegradable polymeric microcapsules for selective ultrasound-triggered drug release.* Soft Matter, 2011. **7**(11): p. 5417-5422.
101. Alvarez-Lorenzo, C., L. Bromberg, and A. Concheiro, *Light-sensitive Intelligent Drug Delivery Systems†.* Photochemistry and Photobiology, 2009. **85**(4): p. 848-860.
102. Brazel, C., *Magnetothermally-responsive Nanomaterials: Combining Magnetic Nanostructures and Thermally-Sensitive Polymers for Triggered Drug Release.* Pharmaceutical Research, 2009. **26**(3): p. 644-656.
103. Kotanen, C.N., et al., *Biomimetic hydrogels gate transport of calcium ions across cell culture inserts.* Biomedical Microdevices, 2012. **(in press)**.
104. Um, S.H., et al., *Enzyme-catalysed assembly of DNA hydrogel.* Nat Mater, 2006. **5**(10): p. 797-801.
105. Van Tomme, S.R., G. Storm, and W.E. Hennink, *In situ gelling hydrogels for pharmaceutical and biomedical applications.* International Journal of Pharmaceutics, 2008. **355**(1-2): p. 1-18.
106. Champion, J.A., Y.K. Katare, and S. Mitragotri, *Particle shape: A new design parameter for micro- and nanoscale drug delivery carriers.* Journal of Controlled Release, 2007. **121**(1-2): p. 3-9.
107. Yoo, J.-W., N. Doshi, and S. Mitragotri, *Adaptive micro and nanoparticles: Temporal control over carrier properties to facilitate drug delivery.* Advanced Drug Delivery Reviews, 2011. **63**(14-15): p. 1247-1256.
108. Yoo, J.-W. and S. Mitragotri, *Polymer particles that switch shape in response to a stimulus.* Proceedings of the National Academy of Sciences, 2010. **107**(25): p. 11205-11210.
109. Kim, J., S. Nayak, and L.A. Lyon, *Bioresponsive Hydrogel Microlenses.* Journal of the American Chemical Society, 2005. **127**(26): p. 9588-9592.
110. Holtz, J.H. and S.A. Asher, *Polymerized colloidal crystal hydrogel films as intelligent chemical sensing materials.* Nature, 1997. **389**(6653): p. 829-832.
111. Yang, Z., et al., *Using β-Lactamase to Trigger Supramolecular Hydrogelation.* Journal of the American Chemical Society, 2006. **129**(2): p. 266-267.
112. Kim, H., et al., *Live Lymphocyte Arrays for Biosensing.* Advanced Functional Materials, 2006. **16**(10): p. 1313-1323.
113. Ma, W.M.J., et al., *Dye displacement assay for saccharide detection with boronate hydrogels.* Chemical Communications, 2009(5): p. 532-534.
114. Zhao, Y., et al., *Quantum-Dot-Tagged Bioresponsive Hydrogel Suspension Array for Multiplex Label-Free DNA Detection.* Advanced Functional Materials, 2010. **20**(6): p. 976-982.
115. Kotanen, C.N., et al., *Implantable enzyme amperometric biosensors.* Biosensors and Bioelectronics, 2012. **35**(1): p. 14-26.
116. Guiseppi-Elie, A., *An implantable biochip to influence patient outcomes following trauma-induced hemorrhage.* J Anal and Bioanal Chem, 2010. **339**(1): p. 403-419.

117. Guiseppi-Elie, A., C. Lei, and R.H. Baughman, *Direct electron transfer of glucose oxidase on carbon nanotubes.* Nanotechnology, 2002. **13**(5): p. 559.
118. Shao, Y., et al., *Graphene Based Electrochemical Sensors and Biosensors: A Review.* Electroanalysis, 2010. **22**(10): p. 1027-1036.
119. Peppas, N.A., et al., *Hydrogels in pharmaceutical formulations.* European Journal of Pharmaceutics and Biopharmaceutics, 2000. **50**(1): p. 27-46.
120. Lin, C.-C. and A.T. Metters, *Hydrogels in controlled release formulations: Network design and mathematical modeling.* Advanced Drug Delivery Reviews, 2006. **58**(12-13): p. 1379-1408.
121. Caldorera-Moore, M. and N.A. Peppas, *Micro- and nanotechnologies for intelligent and responsive biomaterial-based medical systems.* Advanced Drug Delivery Reviews, 2009. **61**(15): p. 1391-1401.
122. Yang, J., et al., *Synthesis of biodegradable multiblock copolymers by click coupling of RAFT-generated heterotelechelic poly(HPMA) conjugates.* React. Funct. Polymers, 2011. **71**: p. 294-302.
123. Westbrook, K.K. and H.J. Qi, *Actuator Designs using Environmentally Responsive Hydrogels.* Journal of Intelligent Material Systems and Structures, 2008. **19**(5): p. 597-607.
124. Vogt, A.P. and B.S. Sumerlin, *Temperature and redox responsive hydrogels from ABA triblock copolymers prepared by RAFT polymerization.* Soft Matter, 2009. **5**(12): p. 2347-2351.
125. Gupta, P., K. Vermani, and S. Garg, *Hydrogels: from controlled release to pH-responsive drug delivery.* Drug Discovery Today, 2002. **7**(10): p. 569-579.
126. Miyata, et al., *Preparation of reversibly glucose-responsive hydrogels by covalent immobilization of lectin in polymer networks having pendant glucose.* Journal of Biomaterials Science, Polymer Edition, 2004. **15**: p. 1085-1098.
127. Tauro, J.R., et al., *Matrix metalloprotease selective peptide substrates cleavage within hydrogel matrices for cancer chemotherapy activation.* Peptides, 2008. **29**(11): p. 1965-1973.
128. Venkatesh, S., J. Wower, and M.E. Byrne, *Nucleic Acid Therapeutic Carriers with On-Demand Triggered Release.* Bioconjugate Chemistry, 2009. **20**(9): p. 1773-1782.
129. Vemula, P.K., et al., *Self-assembled prodrugs: An enzymatically triggered drug-delivery platform.* Biomaterials, 2009. **30**(3): p. 383-393.
130. Kopecek, J.H., *Biomaterials and Drug Delivery: Past, Present, and Future.* Molecular Pharmaceutics 2010. **7**(4): p. 922-925.
131. Wang, C., R.J. Stewart, and J. Kopecek, *Hybrid hydrogels assembled from synthetic polymers and coiled-coil protein domains.* Nature, 1999. **397**(6718): p. 417-420.
132. Ulijn, R.V., *Enzyme-responsive materials: A new class of smart biomaterials.* J. Mater. Chem. , 2006. **16**: p. 2217-2225.
133. Trengove, N.J., et al., *Analysis of the acute and chronic wound environments: the role of proteases and their inhibitors.* Wound Repair and Regeneration, 1999. **7**(6): p. 442-452.

134. Wysocki, A.B., et al., *Temporal expression of urokinase plasminogen activator, plasminogen activator inhibitor and gelatinase-B in chronic wound fluid switches from a chronic to acute wound profile with progression to healing.* Wound Repair and Regeneration, 1999. **7**(3): p. 154-165.
135. McDonald, T.O., et al., *Branched peptide actuators for enzyme responsive hydrogel particles.* Soft Matter, 2009. **5**(8): p. 1728-1734.
136. White, C.J., et al., *Extended release of high molecular weight hydroxypropyl methylcellulose from molecularly imprinted, extended wear silicone hydrogel contact lenses.* Biomaterials, 2011. **32**(24): p. 5698-5705.
137. Jhaveri, S.J., et al., *Release of Nerve Growth Factor from HEMA Hydrogel-Coated Substrates and Its Effect on the Differentiation of Neural Cells.* Biomacromolecules, 2008. **10**(1): p. 174-183.
138. Bradbury, E.J., et al., *Chondroitinase ABC promotes functional recovery after spinal cord injury.* Nature, 2002. **416**(6881): p. 636-640.
139. Moore, K., M. Macsween, and M. Shoichet, *Immobilized Concentration Gradients of Neurotrophic Factors Guide Neurite Outgrowth of Primary Neurons in Macroporous Scaffolds.* Tissue Engineering, 2006. **12**(2): p. 267-278.
140. DelMar, E.G., et al., *A sensitive new substrate for chymotrypsin.* Analytical Biochemistry, 1979. **99**(2): p. 316-320.
141. Liu, S.-Q., et al., *Bio-functional micelles self-assembled from a folate-conjugated block copolymer for targeted intracellular delivery of anticancer drugs.* Biomaterials, 2007. **28**(7): p. 1423-1433.
142. Kalogeris, E., et al., *Properties of catechol 1,2-dioxygenase from Pseudomonas putida immobilized in calcium alginate hydrogels.* Enzyme and Microbial Technology, 2006. **39**(5): p. 1113-1121.
143. Shah, S.S., M.G. Kulkarni, and R.A. Mashelkar, *Release kinetics of pendant substituted bioactive molecules from swellable hydrogels: role of chemical reaction and diffusive transport.* Journal of Membrane Science, 1990. **51**(1-2): p. 83-104.
144. Fournier, R.L., *Basic transport phenomena in biomedical engineering*2007: Taylor & Francis.
145. Brahim, S., D. Narinesingh, and A. Guiseppi-Elie, *Synthesis and Hydration Properties of pH-Sensitive p(HEMA)-Based Hydrogels Containing 3-(Trimethoxysilyl)propyl Methacrylate.* Biomacromolecules, 2003. **4**(3): p. 497-503.
146. Abraham, S., et al., *Molecularly engineered p (HEMA)-based hydrogels for implant biochip biocompatibility.* Biomaterials, 2005. **26**(23): p. 4767-4778.
147. Karageorgiou, V. and D. Kaplan, *Porosity of 3D biomaterial scaffolds and osteogenesis.* Biomaterials, 2005. **26**(27): p. 5474-5491.
148. Achstetter, T., C. Ehmann, and D.H. Wolf, *New proteolytic enzymes in yeast.* Archives of Biochemistry and Biophysics, 1981. **207**(2): p. 445-454.
149. Perona, J.J., et al., *Structural origins of substrate discrimination in trypsin and chymotrypsin.* Biochemistry, 1995. **34**(5): p. 1489-1499.

150. Wesolowska, O., et al., *Enhancement of chymotrypsin-inhibitor/substrate interactions by 3 M NaCl.* Biochimica et Biophysica Acta (BBA) - Protein Structure and Molecular Enzymology, 2001. **1545**(1-2): p. 78-85.
151. Cheng, M.-L. and Y.-M. Sun, *Observation of the solute transport in the permeation through hydrogel membranes by using FTIR-microscopy.* Journal of Membrane Science, 2005. **253**(1-2): p. 191-198.
152. Rutherford, S.W. and D.D. Do, *Review of time lag permeation technique as a method for characterisation of porous media and membranes.* Adsorption, 1997. **3**(4): p. 283-312.
153. Fogler, H.S., *Elements of chemical reaction engineering*2006: Prentice Hall PTR.
154. Truskey, G.A., F. Yuan, and D.F. Katz, *Transport phenomena in biological systems*2009: Pearson Prentice Hall.
155. Segev, O., et al., *Probing the Molecular Interaction of Chymotrypsin with Organophosphorus Compounds by 31P Diffusion NMR in Aqueous Solutions.* The Journal of Organic Chemistry, 2004. **70**(1): p. 309-314.
156. Pastor, I., et al., *Diffusion of α-Chymotrypsin in Solution-Crowded Media. A Fluorescence Recovery after Photobleaching Study.* The Journal of Physical Chemistry B, 2010. **114**(11): p. 4028-4034.